Journal of Volcanology and Geothermal Research 333-334 (2017) 36–52

Contents lists available at ScienceDirect

Journal of Volcanology and Geothermal Research

journal homepage: www.elsevier.com/locate/jvolgeores

Spatio-temporal evolution of rockfall activity from 2007 to 2011 at the Piton de la Fournaise volcano inferred from seismic data

Clément Hibert[a,b,d,*], Anne Mangeney[a], Gilles Grandjean[b], Aline Peltier[c], Andrea DiMuro[c], Nikolai M. Shapiro[a], Valérie Ferrazzini[c], Patrice Boissier[c], Virginie Durand[a], Philippe Kowalski[c]

[a] Institut de Physique du Globe de Paris, Paris, Sorbone Paris Cité, Université Paris Diderot, UMR 7154 CNRS, France
[b] Bureau des Recherches Géologiques et Minières, DRP/RIG, Orléans, France
[c] Observatoire Volcanologique du Piton de la Fournaise/Institut de Physique du Globe de Paris, Sorbone Paris Cité, La Plaine des Cafres, Réunion, France
[d] Institut de Physique du Globe de Strasbourg/EOST, Strasbourg, UMR 7516 CNRS, France

ARTICLE INFO

Article history:
Received 6 September 2016
Received in revised form 6 December 2016
Accepted 6 January 2017
Available online 11 January 2017

Keywords:
Rockfalls
Volcano-seismology
Volcano
Piton de la Fournaise
Volcano monitoring

ABSTRACT

Seismic data have been used to catalog the location and volume of most of the rockfalls that occurred at the Piton de la Fournaise volcano from May 2007, just after the major collapse of the Dolomieu summit crater floor, to May 2011. This catalog made it possible to compare the evolution of the number and volume of rockfalls at a high temporal resolution and to investigate their links with eruptions, seismicity, deformations and rainfalls affecting the Piton de la Fournaise volcano. Results show that the purge of unstable areas created by the Dolomieu crater floor collapse occurred in two phases: a first phase, lasting three months, during which the intense rockfall activity immediately following the collapse decreased abruptly and a second phase, lasting more than two years, during which the daily volume of the rockfalls slowly decreased before reaching a steady state. A detailed study of 4 time periods, including 3 eruptive cycles, indicates that strong seismicity can increase the number of rockfalls. Furthermore, when a dike reaches the surface at the summit of the central cone, giving birth to an eruption, the associated local forcing can in some cases increase the volume of rockfalls, possibly by creating or expanding weak zones. In most cases, this is not observed for dike intrusions that do not reach the surface. The newly created weak zones are most often far from the eruptive fissures of the ongoing eruption, but close to the location of the next eruption. This suggests that these distant zones are also weakened at depth, thus creating preferred paths for future dikes propagating toward the surface. The impact of rainfall on rockfall activity was also studied, given that La Réunion Island is subject to very intense rainfall events. Our results show that rainfall can in some cases trigger rockfalls rapidly, with response times of less than a day, but not systematically, and no triggering rainfall threshold was found.

1. Introduction

Volcanoes are among the most dynamic geological phenomena on Earth. Continuous deformation and other processes affecting the surfaces of volcanoes can potentially trigger gravitational instabilities. While gravitational instabilities occurring on volcanoes may take many forms, several dramatic examples in recent decades have shown the strong hazard potential of slope destabilization during or between eruptive periods. The iconic eruption of Mount St. Helens in 1980 is probably the best known example of the link between volcanic activity and slope failure, representing one of the biggest landslides observed in recent history (2.5×10^9 m^3) (Kanamori and Given, 1982; Kanamori et al., 1984). A more recent example of the damage potential of gravitational instabilities in a volcanic context is the collapse of part of the Stromboli volcano flank during the 2002 eruption (Bonaccorso et al., 2003; La Rocca et al., 2004; Calvari et al., 2005; Acocella et al., 2006). There, two successive landslides occurred 7 min apart, with volumes estimated to be approximately 30×10^6m^3, generating a tsunami that damaged structures along the coast of Sicily and Calabria. On La Réunion Island, rockfalls associated with the initial destabilization caused by the 1965 Mahavel landslide (30×10^6m^3), which resulted in the complete evacuation of the village of Roche-Plate and formed a lake of mud (Dupon, 1984; Stieltjes, 1990), have displaced millions of cubic meters of material between 1996 and 2001 (Rousseau, 1999).

Beyond these catastrophic events, smaller gravitational events also pose a threat and may in addition carry information on volcano unrest and possible eruptive or intrusive processes. Several authors have shown that rockfall activity is correlated with the growth of steep and unstable lava domes observed at andesitic volcanoes such

* Corresponding author at: EOST/Université de Strasbourg, France. Tel.: +33 845 365 8435.
E-mail address: hibertclement@gmail.com (C. Hibert).

http://dx.doi.org/10.1016/j.jvolgeores.2017.01.007
0377-0273/

as Merapi (Indonesia) or the Soufriere Hills volcano (Montserrat island). These rockfalls originate from the fracturing of the outer shell of the growing lava dome, composed of cooled and degassed lava. The intensity of the rockfall activity and the propensity that the lava dome can have to collapse and generate a pyroclastic flow can be correlated with the rate of extrusion of the magma (Calder et al., 2005). Using a probabilistic approach, Calder et al. (2005) showed that during extrusion periods, the occurrence of rockfalls was an indicator of the rate of extrusion. A similar conclusion was also found by Ui et al. (1999) for the eruptions of Unzen (Japan) from 1990 to 1995. Thus, the rockfall activity can be an important precursor to the next occurrence of a pyroclastic flow. As shown by several authors for the case of the Soufriere Hills volcano, rockfall activity is also spatially correlated with directional changes of the extrusion lobes (Watts et al., 2001) and temporally correlated with changes in the type of eruptions (Calder et al., 2002). An increase in the activity of rockfalls is observed immediately after the arrival of new inputs of magma at the base of the volcanic edifice (Voight et al., 1999). For the 1994 eruption of the Merapi volcano, Voight et al. (2000) found a significant increase in rockfall activity a few hours before the lava dome collapse.

Only a few studies have focused on the relationship between eruptive activity and rockfall activity for basaltic volcanoes. Orr et al. (2013) showed that rockfalls coming from the crater rim of Halemaumau pit crater and falling into the lava lake formed during the 2008–2010 eruption of the Kilauea Volcano (Hawaii) could change the eruptive regime. Most of the time, only minor ejections of matter from the lava lake were observed, however significant explosive activity was observed when rockfalls impacted and destabilized the surface of the lava lake. Falsaperla et al. (2006) showed that since the catastrophic flank collapse on Stromboli in 2002, an area located close to the landslide scarp has been very active in terms of generating gravitational instabilities. The authors of that study concluded that, if the progressive degradation continued to spread to the main crater, it could create a sudden depressurization of the volcanic conduit and thus quickly change the eruptive activity of the Stromboli volcano (Falsaperla et al., 2008).

These studies highlight the need for continuous monitoring of gravitational instabilities in volcanic contexts, including their volume and location, to provide information on fast changes in the eruptive regime of volcanoes. In the present study, we investigate the relationship between rockfall activity in the Dolomieu caldeira, which is the main summit structure of the Piton de la Fournaise volcano, and external forcings, with a particular focus on the influence of volcanic activity. We use continuous seismic records and seismology-based methods to assess retrospectively the number and volume of the rockfalls that occurred between May 2007 and May 2011. The aim of our study is twofold: i) to use the seismic data collected on rockfalls to study the spatio-temporal evolution of these events and the impact of external forcing such as the deformation generated by eruptions and intrusions, the induced seismicity, and rainfall events; ii) to determine if rockfall activity may provide information on the outcome of intrusive processes and volcano unrest in general.

In the first section we present the geological context of our study. The second section presents the seismology-based methods and the processing chain we use to construct our catalog that contains the number, volume and location of rockfalls. We then focus on the global trend of the rockfall activity and the potential correlations with long-term eruptive cycles of the Piton de la Fournaise volcano. Then, in the fourth section, we take a closer look at three eruptive periods and the period just following the Dolomieu crater floor collapse of April 2007 to determine the temporal and spatial evolution of the number and volumes of rockfalls and their relationship with eruptive activity. Finally, in the last section, we discuss the possible impacts of eruptive processes and rainfall on rockfall activity.

2. Context and rockfall observation

2.1. Geological context: The Piton de la Fournaise volcano and the April 2007 Dolomieu crater floor collapse

The Piton de la Fournaise volcano is a basaltic volcano that constitutes the southeastern part of La Réunion Island (Indian Ocean), located 800 km east of Madagascar. La Réunion is the youngest of the islands created by the Deccan Trapps hotspot (Duncan, 1981). Two volcanic structures are visible on La Réunion Island today: The largest is Piton des Neiges, which last erupted 12,000 years ago (Deniel et al., 1992), and Piton de la Fournaise, which is still active, with an eruption every 8 months on average over the last 50 years (Peltier et al., 2009a; Roult et al., 2012; Staudacher et al., 2009), making it one of the most active basaltic volcanoes in the world. The central cone is located within a caldera named “Enclos Fouqué”, that was formed 4500 years ago (Bachèlery, 1981). The majority of recent eruptions have occurred within this caldera (e.g. Roult et al., 2012). The activity of Piton de la Fournaise is characterized by fissure eruptions fed by a magma reservoir located near sea level (Fukushima et al., 2005; Peltier et al., 2007, 2008) . The present day summit shows two collapsed structures named the Bory crater, which is currently inactive, and the Dolomieu crater, within which numerous eruptions occur (Fig. 1). A detailed description of both structures and of the internal cliffs is found in Peltier et al. (2012) and Michon et al. (2013). A major eruption occurred on April 2007 leading to the collapse of the floor of the Dolomieu crater. This event marks the beginning of our period of interest.

The eruption started on 2 April 2007 in the east-south-east part of the Enclos Fouqué at an elevation of 590 m. The length of the eruptive fissure was estimated to be 1 km and lava fountains with heights ranging from 100 to 150 m were observed, attesting to the extreme intensity of this eruption (Staudacher et al., 2009). The total volume of the emitted lava was estimated to be approximately 240×10^6 m^3 (Bachèlery et al., 2010). This eruption led to the largest crater floor collapse since the beginning of observations at Piton de la Fournaise (i.e. since 1760). Ground deformation and seismic data make it possible to date the beginning of the collapse at around 20:48 (GMT) on 5 April 2007 (Staudacher et al., 2009). The first direct observations of the collapse were made only on 6 April, 16 h after the first seismic records.

Direct observations revealed that the Dolomieu crater floor collapse initially affected the northern part of the crater and then extended westward, leaving two plateaus to the south and east parts, which correspond to the former crater floor (Michon et al., 2007). On 10 April 2007, the newly formed caldera stretched to the dimensions of the pre-existing crater (1100 m long and 800 m wide), and was deepened by 340 m with respect to the former elevation of the crater floor. The total collapsed volume was estimated to be between 90×10^6 m^3 and 100×10^6 m^3 (Michon et al., 2007; Urai et al., 2007; Staudacher et al., 2009; Peltier et al., 2009b). Since this major event, the edges of the Dolomieu crater have been considerably destabilized and numerous rockfalls have been observed.

Between the Dolomieu crater collapse in April 2007 and May 2011, 8 eruptions, with eruptive fissures opening and lava extrusion observed at the surface, occurred (Roult et al., 2012). The dates, durations and distances from the Dolomieu crater of the 8 eruptions are presented in Table 1 and their locations are marked in Fig. 1a. Eruptions at Piton de la Fournaise are usually preceded by an increase in seismic activity and deformation in the months to days prior to the eruption. Seismic activity and ground deformation abruptly increases when a dike migrates, giving rise to a succession of volcano-tectonic earthquakes. This rapid succession of VT is called a seismic crisis (Collombet et al., 2003; Peltier et al., 2005; Peltier et al., 2009a; Lengliné et al., 2008). Usually, these events are located below the central cone, with depths ranging from 0 to 2300 m above

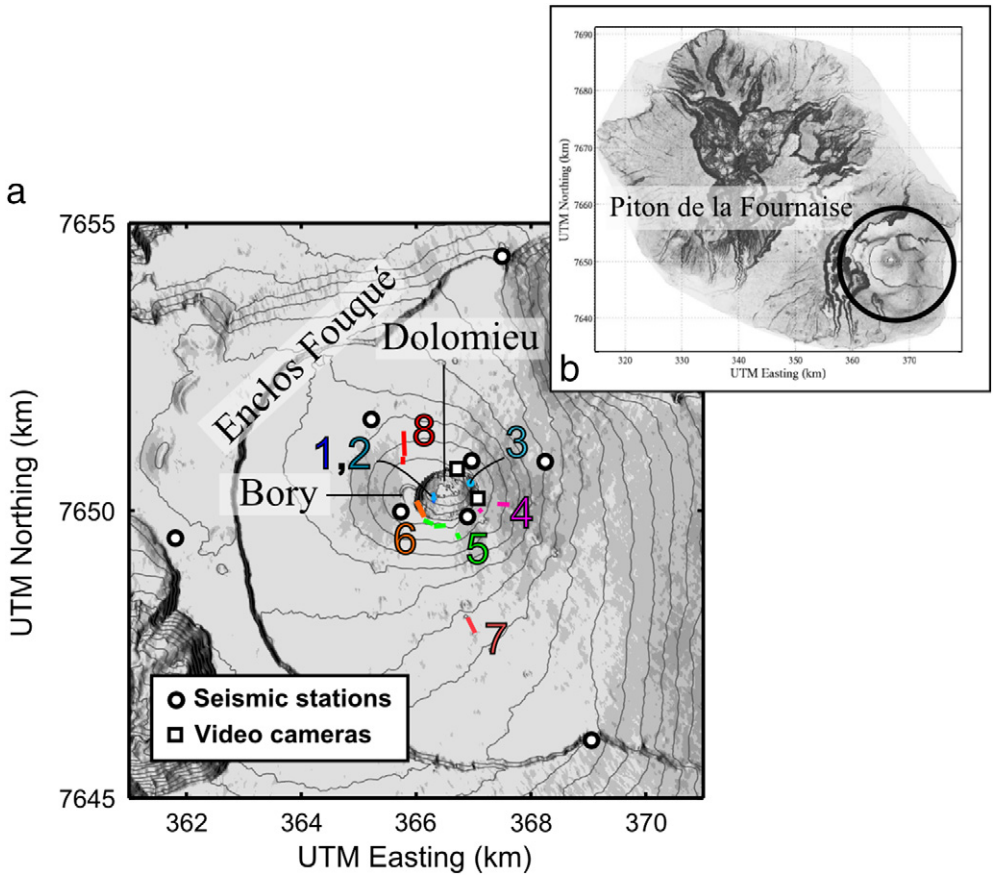

Fig. 1. a) Map of the Piton de la Fournaise volcano and location of the eruptive fissures of the eight eruptions that occurred from 2008 to 2010. The dates of occurrence of the eruptions are indicated in Table 1. b) Piton de la Fournaise on La Réunion Island.

sea level (Battaglia et al., 2005; Massin et al., 2011; Taisne et al., 2011; Roult et al., 2012). This crisis is followed by a quiet period and then by seismic tremor associated with the beginning of the surface eruptive activity. However, in the majority of cases, seismic crises are not followed by eruptions. 18 non-eruptive seismic crises were recorded in the study period. During an intrusion, a dike or a sill propagates within the volcano structure and also generates a seismic crisis and deformation, but stops before reaching the surface and therefore does not qualify as an eruption. Before the April 2007 crater floor collapse, intrusions were a rare phenomenon at the Piton de la Fournaise volcano. The increase in the number of intrusion may be due to the reorganization of the stresses in the volcanic edifice consecutive to the April 2007 crater floor collapse which should tend to limit dike propagation below the surface (Peltier et al., 2010; Roult et al., 2012). Non-eruptive seismic crises may also be related to deep intrusions or brittle failure associated with hydrothermal fluids, but in the absence of deformation recorded at the surface the nature of these event cannot be confirmed (Roult et al., 2012). Thus, since the April 2007 eruption, it has become challenging to discriminate seismic crises which will evolve onto eruptive events from non-eruptive seismicity.

Table 1
Starting date, duration, approximate distance D_{Dol} to the center of the Dolomieu crater and extruded lava volume of the 8 eruptions that occurred between 2008 and 2010 (after Roult et al. (2012)).

#	Starting date	Duration (days)	D_{Dol} (m)	Volume (Mm^3)
1	21/09/2008	11	100	1
2	27/11/2008	1	100	0.1
3	15/12/2008	52	300	1.5
4	5/11/2009	1	500	0.14
5	14/12/2009	1	600	0.16
6	02/01/2010	10	500	1.6
7	14/10/2010	17	2100	2.7
8	09/12/2010	0.5	900	0.5

2.2. Rockfalls in the Dolomieu crater: observation

Immediately after the collapse of the Dolomieu crater floor, the number of rockfalls increased considerably. Most of the time, the rockfalls departed from the highly fractured edges of the Dolomieu crater. For the 2007–2011 period, the main transport process of the material displaced by rockfalls was granular flow (Hibert et al., 2011). In order to directly observe the rockfalls, two seismically triggered video cameras were installed in April 2010 at the summit of Piton de la Fournaise. The combined view angles of the two cameras cover the southern and western part of the Dolomieu crater (Fig. 1b). Both cameras buffer one day of data, with a sampling rate of two images per second. The seismic signals generated by rockfalls are identified and dated every day at the Observatoire Volcanologique du Piton de la Fournaise (OVPF). The date information is returned to the cameras and then the images for the indicated period are sent back to the observatory. This device produced several movies of rockfalls that we then compared to the associated seismic signals and spectrograms. Fig. 2 shows an example recorded on 23 September 2011.

The first moving particle visible to human eyes was observed just one second after the onset detected on the seismic signal (Fig. 2d). It seems from visual observations that the increasing phase of the amplitude of the seismic signal corresponds to the period during which the volume of material displaced on the slope and the velocity of the bulk of the granular flow were increasing (Fig. 2e). The largest

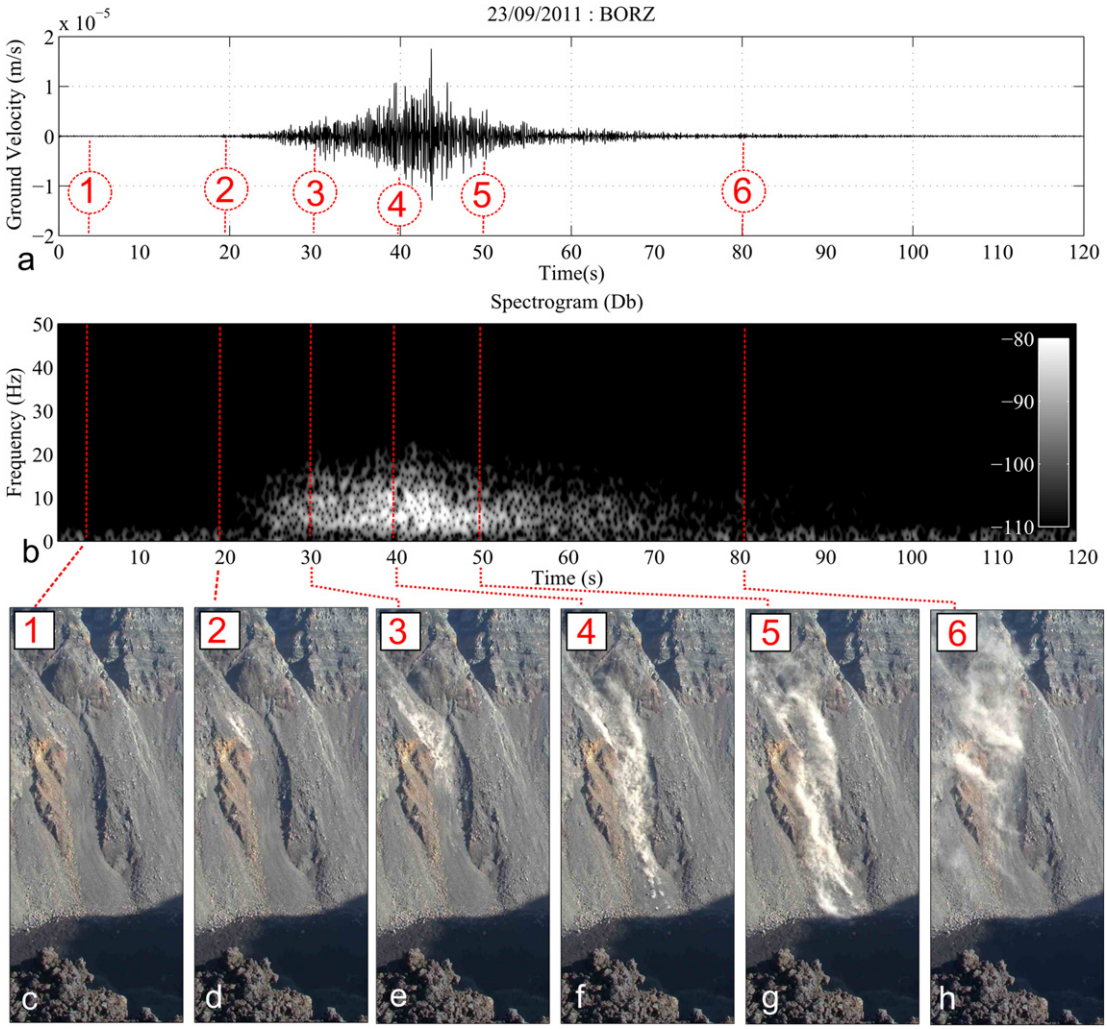

Fig. 2. a) Seismic signal and b) spectrogram generated by the 23/09/2011 rockfall. Still images extracted from the movie for times (local): c) t=12:09:59; d) t=12:10:15; e) t=12:10:26; f) t=12:10:37 g) t=12:10:47 and h) t=12:11:17.

moving rocks were observed on the slope at the front of the flow during this phase (Fig. 2f). After the seismic peak amplitude, there was still a strong emission of dust (Fig. 2g), which suggests that a part of the mass was still flowing on the slope. Finally, the moment when the last moving particle was observed and when the emission of dust stopped, corresponds to within a few seconds to the time when the seismic signal amplitude reached the pre-event noise level (Fig. 2h).

The joint observation of the movie and the seismogram for the 23 September rockfall shows that the physical process that generated the seismic wave was the propagation of the granular flow along the slope. The seismogenic process was completely dominated by the propagation phase of the granular flow. This joint observation also confirms the hypothesis proposed by Hibert et al. (2011), that the duration of the seismic signals recorded at nearby stations is approximately the same as the propagation time of the granular flow along the slope.

3. Methods: constructing the rockfall catalog

The seismic catalog we use in this study is derived from the initial catalog provided by OVPF. This initial catalog is based on a STA/LTA detector (Allen, 1982) that receives the continuous seismic records provided by the seismic stations network deployed on the Piton de la Fournaise volcano. A manual identification of the seismic source of the events is performed daily for each detected event and is based on the knowledge and the expertise of the operator. Several types of events generate seismic waves recorded by the seismic network of OVPF and among them the two dominant classes are rockfalls and volcano-tectonic earthquakes (VT). VT can be caused by to the propagation of dikes within the volcanic edifice and more generally by stress changes at depth related to magma movement, pressurization or hydrothermal fluids. The information given by this catalog includes the time of occurrence of the events, the magnitude of the VT earthquakes and the duration of the signal for all classes of events. The distribution of the duration of all the rockfalls in our data-set is presented in Fig. 3. The values range from 10 to 300 s, with a mean duration of 53 s, in the range of what was observed at the Soufrière Hills volcano on Montserrat (Calder et al., 2005) or at Volcan de Colima (Zobin et al., 2008; Mueller et al., 2013) for example.

To locate the rockfalls, we use the two-step processing chain developed by Hibert et al. (2014). We based our analysis on signals recorded at 8 short-period seismic stations (Marck Product L4C 1Hz), with distances to the Dolomieu crater ranging from 300 m to 5 km(Fig. 1b). First, the onset of the seismic signal generated by a rockfall is accurately picked at each station using a kurtosis-based method (Baillard et al., 2014; Hibert et al., 2014) . Then, the picked times are processed by a locating method based on propagation models built using a Fast Marching Method (e.g. Sethian, 1996a,b,c) that

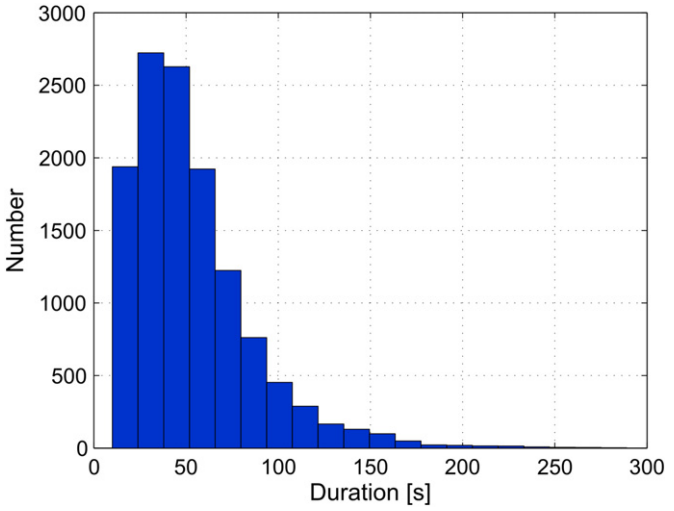

Fig. 3. Histogram of the distribution of the rockfalls duration in the entire data-set.

construct a hyperbola for each pair of stations that have recorded a signal. The hyperbolas are stacked and their focal point provides the optimal location of the source. The uncertainty in the picking of the first arrivals and of the locating process are taken into account and provide an estimate of the spatial location error.

To complete this catalog with relevant information regarding rockfall activity, we determined the volumes of each rockfall. Their volume can be derived from the energy of the seismic signal generated by the rockfall using the formula proposed by Hibert et al. (2011):

$$V = \frac{3E_s}{R_{s/p}.\rho g L \cos\theta \left(\left|\tan\theta - \tan\alpha\right)\right|}, \quad (1)$$

where $R_{s/p}$ is the mean ratio between seismic energy and potential energy lost by rockfalls occurring in the Dolomieu crater, ρ the density of the granular mass, g gravitational acceleration, L the average length of the slope over which the rockfalls occur, θ the mean slope angle, α the repose angle of the deposit on the slope and E_s the energy of the seismic signal. A first approximation of the seismic energy E_s, assuming an isotropic homogeneous propagation medium and a point-force source, and that surface waves dominate the seismic signals, is given by:

$$Es = \int_{t_2}^{t_1} 2\pi r \rho h c \, u_{env}(t)^2 e^{\alpha r} dt \quad (2)$$

with:

$$u_{env}(t) = \sqrt{u(t)^2 + Ht(u(t))^2} \quad (3)$$

where t_1 and t_2 are respectively the picked onset and final times of the seismic signal, r is the distance between the event and the recording station, h is the thickness of the layer through which surface waves propagate, ρ the density of the ground, and c is the group velocity of the seismic waves (Crampin and Båth, 1965; Vilajosana et al., 2008). $u_{env}(t)$ is the amplitude envelope of the seismic signal (here the ground velocity) obtained using the Hilbert transform (Ht), and α is a damping factor that accounts for anelastic attenuation of the waves (Aki and Richards, 1980) (see Hibert et al. (2011)) for details concerning the values assigned to each parameter in Eqs. (1) and (2).

The initial OVPF catalog included 12,422 rockfalls for the period extending from May 2007 to May 2011. To accurately compute the seismic energy and thus the volume of a given rockfall, we need to know its location. We choose to include in our catalog only rockfalls with low location errors to ensure an acceptable uncertainty for the volume computation. The average spatial error of the rockfalls we selected is approximately 180 m (Hibert et al., 2014). For a given rockfall, the processing steps involve picking the first-arrivals of the seismic signals, locating the event and, if the location uncertainty is low enough, computing the seismic energy and the volume. From the initial catalog including 12,422 rockfalls, we kept 8152 events. The discarded events are likely to be the smaller ones. The two causes of high location uncertainty are a lack of records at a sufficient number of stations (typically 3 or more) or a poor signal-to-noise ratio of the seismic signals. The lack of good records on a significant number of stations or a poor signal-to-noise ratio are generally due to low seismic signal amplitude, which is directly linked to the volume of material displaced by the event (Hibert et al., 2011).

4. Global trend of rockfall activity for the May 2007–May 2011 period

Time series showing the temporal evolution of the daily number of rockfalls (Fig. 4a) and the daily rockfall volumes (Fig. 4b) have been computed from the catalog. The most active period, in terms of both the number of rockfalls occurring and the volumes of material displaced, is the one immediately following the collapse of the Dolomieu crater (Fig. 4a and b). Numerous large events occurred during this period when, according to deformation data, the Dolomieu crater edges underwent a post-collapse subsidence. A third of the total volume estimated for the 2007–2011 period, estimated to be 3.23×10^6 m^3 (Fig. 4d), was displaced before 7 June 2007 and half before 5 July 2007. The volume and the number of rockfalls decreased following a rough exponential trend during this first period, similar to an Omori law observed for Earthquakes aftershocks (Hirata, 1987). This behavior was already observed, for Earthquakes induce landslides (e.g. Marc et al., 2015) or after large slope destabilizations (e.g. Wieczorek et al., 1995) for example.

This period of intense rockfall activity ended in July 2007 and was followed by a progressive decrease in activity. After January 2008, the cumulative number of rockfalls followed a linear trend, except for the eruptive periods when the number of rockfalls accelerated (Fig. 4c). The cumulative volume slowly decelerated after July 2007 before reaching a plateau in January 2010. This suggests that there was a second phase of post-collapse relaxation of the Dolomieu crater that lasted for years but had an impact only on the volume of the rockfalls. In other words, the number of rockfalls remained almost constant outside of eruptive periods while the average volume of individual rockfalls decreased from 408 m^3 to 19 m^3.

To complete this global analysis of rockfall activity, we looked at relative changes over time scales of several months. Our goal was to determine whether an eruptive cycle (defined by a succession of seismic crises, intrusions and eruptions) disrupts the normal rockfall activity over the long term. To do so, we computed the average values of the daily number and volumes of rockfalls in two moving windows starting at the same date, one covering 15 days and the other covering 6 months. Then, the ratio of these two moving average series was calculated.

These two graphs show a correlation between the eruptive activity and the activity of rockfalls. There is clearly a relative increase in the daily number of rockfalls during the eruptive periods (Fig. 4e). There is also a relative increase in the daily volume of the rockfalls during eruptive periods, although weaker and decreasing in time during the progressive stabilization of the Dolomieu crater (Fig. 4f). Finally, some peaks on the relative daily volume curve, such as in February 2008, occurred outside these eruptive periods and are

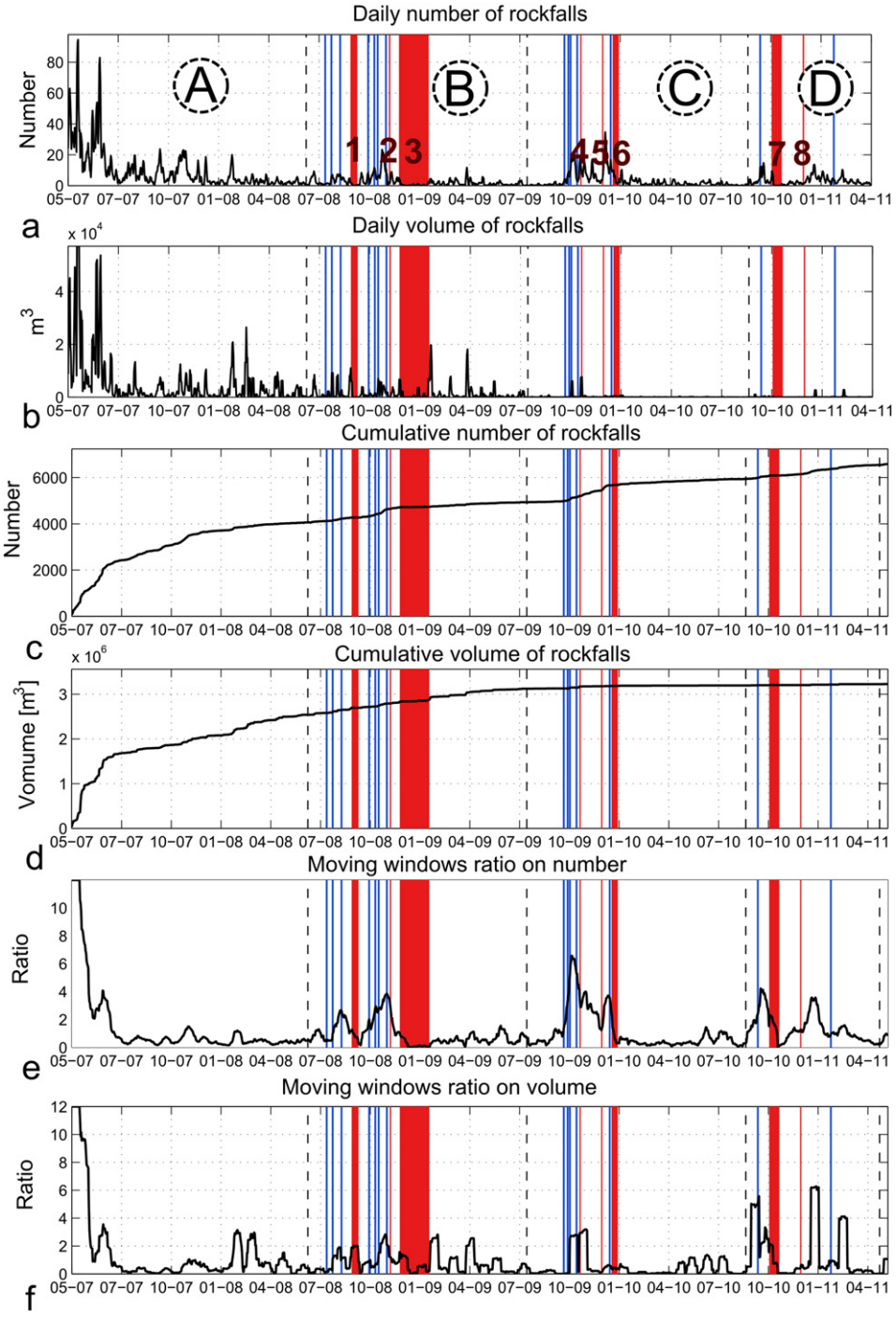

Fig. 4. a) Number of rockfalls per day for the studied period (2007–2011) after the collapse of the Dolomieu crater floor. Eruptions are indicated by red bars and non-eruptive seismic crises, including intrusions, by blue bars. The capital letters indicate the periods studied in detail in the following section. b) Daily sum of rockfall volumes. c) Cumulative sum of the daily number of rockfalls. d) Cumulative sum of the volumes of the rockfalls. e) Ratio of the moving averages (windows of 15 over 180days) of the daily number of rockfalls. f) Ratio of the moving averages (windows of 15 and 180days) of the daily rockfall volumes.

seemingly due to meteorologic activity as discussed in Section 5.1. These eruptive periods will need to be looked at more closely to accurately assess the impact of eruptions, intrusions and seismic crises on the activity of rockfalls.

5. Spatio-temporal evolution of rockfall activity and interaction with different forcings

To observe in more detail the interactions between deformation of the Dolomieu crater, eruptions, seismic crises and rockfall activity, we defined four periods: the first period immediately followed the collapse of the Dolomieu crater floor of April 2007 (period A), and three successive eruptive periods (B, C and D), each including several eruptions and seismic crises. These periods are indicated by their respective letters in Fig. 4a. For each of these periods, we look more specifically at the temporal evolution of the daily number and volume of rockfalls. Note that rockfall seismic signals can be detected during eruptions (e.g. Hibert et al., 2015), however the volcanic tremor can mask the smallest events and perturb the computation of the seismic energy, so we do not comment on the rockfall activity

occurring during the eruptions. To estimate the average volume of rockfalls that occurred on a given day, the ratio between the total volume and the number of rockfalls occurring each day was computed. We also included in our analysis the deformation of the central cone recorded by the SNEG GNSS (Global Navigation Satellite System) station, co-located with the SNE seismic station, very close to the edge of the Dolomieu crater (Fig. 1a). This station was chosen because among those close to the Dolomieu crater, it was the one that gathered the most complete set of data for the period of study. We also gathered the rainfall data recorded at station SNE. Finally, we looked at the location of the rockfalls and the spatial distribution of the seismic energy for some specific sequences within the four periods.

5.1. Temporal evolution

5.1.1. Period A: from May 2007 to June 2008

The period May–June 2007 that immediately follows the collapse of the Dolomieu crater was the most intense in terms of rockfall activity (Fig. 5). It was during these months that the maximum daily volume of material displaced was reached with a cumulative value of 189×10^3 m^3. During this same period, an average of 22 rockfalls per day occurred with an average volume per event of 650 m^3 (Fig. 5a, b and c). The activity then started to decrease, reaching a stable level with an average number of 5 rockfalls per day with a mean volume approaching 240 m^3.

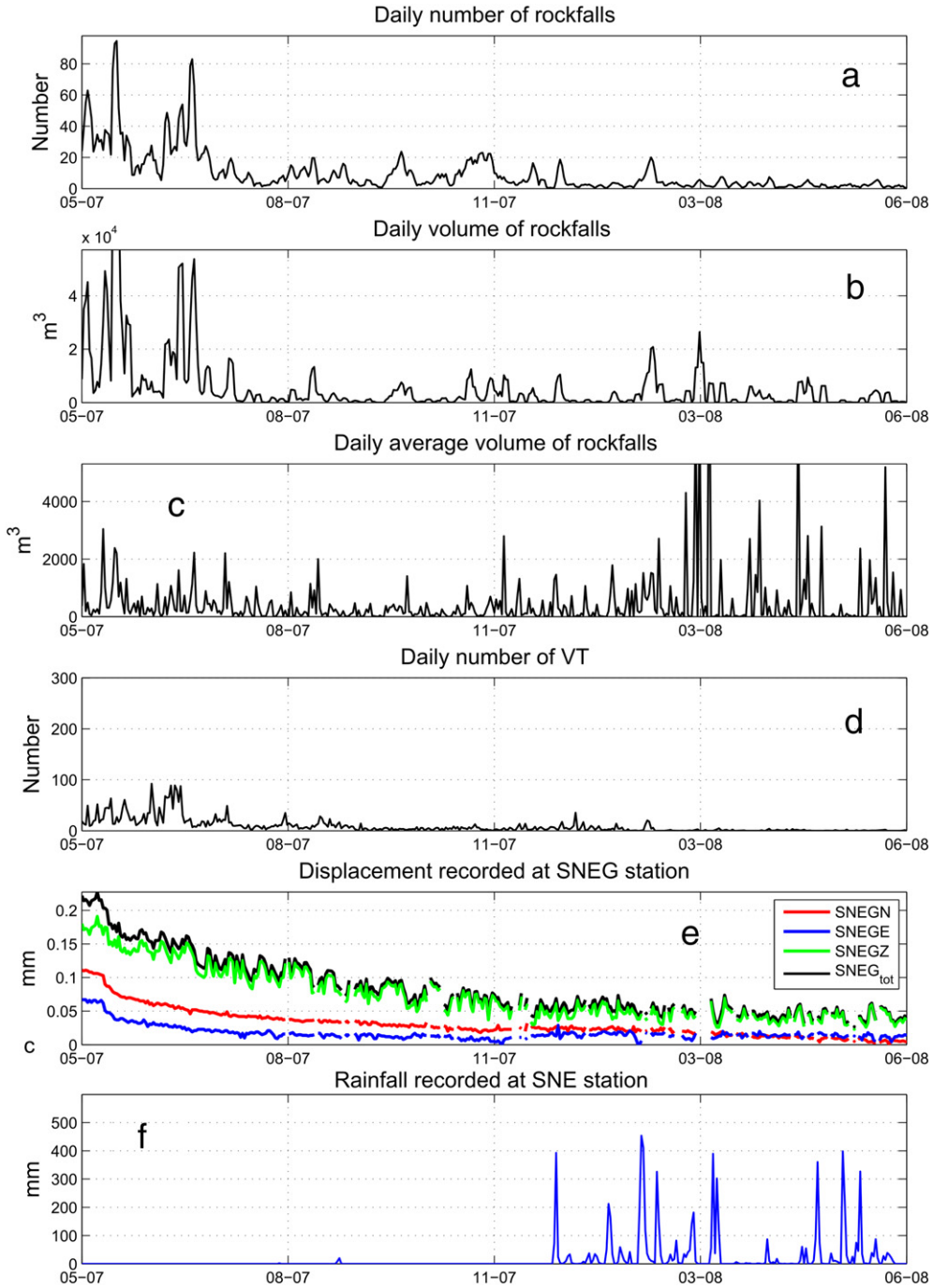

Fig. 5. a) Number of rockfalls per day for period A. b) Total volume of all the rockfalls that occurred on a given day. c) Daily volume divided by the daily number of rockfalls. d) Number of volcano-tectonic earthquakes per day. e) Displacements recorded by different components of the SNEG GNSS station SNEG and total displacement (in black). f) Rainfall recorded at SNE station at the summit of Piton de la Fournaise volcano.

Sporadic peaks of activity can be seen in February and March 2008 when no strong deformation was observed. These episodes are characterized by a low number of rockfalls per day, but with large daily volumes of material displaced, up to 35×10^3 m^3. Three intense tropical cyclones passed close (less than 500 km) from Reunion Island. Cyclone Hondo, Ivan and Lola occurred respectively between 4 and 24 February, 7 and 17 February, and 20 February and 26 March 2008. The strong winds and heavy rainfalls that accompanied these phenomena could have triggered these peaks of activity. It is also important to note that this was the first cyclone season following the collapse of April 2007, which might explain the large impact it seems to have had on the activity of rockfalls in comparison to the following cyclone seasons.

5.1.2. Period B: from July 2008 to July 2009

Three eruptions, the first ones since the Dolomieu crater floor collapse and eleven seismic crises (including four intrusions) occurred during this period. The average volume of rockfalls during this period was 408 m^3 and the maximum daily average volume was 2×10^4 m^3. An increase in the number and volumes of rockfalls was visible before eruptions (1) and (3) (Fig. 6 a, b and c). The volumes of material displaced during the three days preceding eruptions (1) and (3) were 1.1×10^4 m^3 and 7×10^3 m^3 respectively. Eruption (2) was not immediately preceded by any intensification of rockfall activity. Eruptions (1) and (2) occurred within the Dolomieu crater, at the bottom of the cliff that marks the border with the Bory crater (see Fig. 1a for location). In the weeks preceding eruptions (1) and (3), a small and relatively slow continuous horizontal deformation was recorded at SNEG station. Conversely no deformation was observed before eruption (2) (Fig. 6e) that was almost co-located with eruption (1). Even though horizontal deformation was recorded at other GNSS stations located in the vicinity of the summit (Staudacher, 2010; Peltier et al., 2010), no significant horizontal deformation was recorded at the basal GNSS stations and no vertical displacement at any stations before eruption (2). This suggests that the magma supplying this eruption was already at a shallow depth (Di Muro et al., 2015) and reached the surface through a more or less open conduit (Peltier et al., 2010).

Of the 11 seismic crises, 9 coincided with an increase in the daily number of rockfalls but no significant increase in the daily volume was found for most of them. For the 9 seismic crises that coincided with a peak in the number of rockfalls, the largest recorded VT earthquake magnitude during these associated seismic crises exceeds 2. For the first seismic crisis that was not concurrent with a significant increase of the rockfall number, the highest magnitude was 1.01. This suggests that during a seismic crisis, when earthquakes occur at shallow depth beneath the summit, rockfalls can be triggered by the ground acceleration generated by the local earthquakes with the highest magnitudes.

Finally, most of the strong peaks of rockfall activity (both in terms of number and volumes of rockfalls) outside the periods close to eruptive activity seem to be correlated with rainfall peaks (Fig. 6f). This is especially the case for some of the largest peaks occurring before the first seismic crisis and during the weeks that followed eruption (3). The high increase in the number and volume of rockfalls that occurred just after the end of eruption (2) also coincides with a rainfall peak. However several important rockfall activity peaks are not associated with external forcings and might be spontaneous collapses under the effect of gravity.

5.1.3. Period C: from August 2009 to August 2010

Three summit eruptions occurred during this period. They were preceded by a strong surface deformation recorded on the north component of the SNEG GNSS station, indicating that a pressure source was located to the south of the station, below the Dolomieu crater. The average volume of rockfalls during this period was 33 m^3 and the maximum daily average volume was 2×10^3 m^3. Eruption (4) was preceded by an increase in the number and volumes of rockfalls. A very high peak can be seen on the daily volume curve (Fig. 7b) and on the average volume curve (Fig. 7c) one day before the beginning of the eruption.

The behavior of rockfall activity in connection with eruptions (5) and (6) is more difficult to interpret. There are no rockfall activity peaks before eruption (5). However, this eruption was followed by an increase in the number and volumes of rockfalls. This is also the case a few days after eruptions (4) and (6). We do not find any significant increase in rockfall activity before eruption (6), but this activity was already high, probably due to the influence of eruption (5).

All except one of the seismic crises of this period, which qualified as an intrusion, coincided with an increase in the number but not in the volumes of rockfalls (Fig. 7). The maximum magnitudes of the VT earthquakes that occurred during these seismic crises range from 1.86 to 2.11. The intrusion of 18 October 2009, accompanied by an increase in the number and volumes of the rockfalls, represents a very particular event as degassing was observed at the summit of the Piton de la Fournaise volcano, suggesting the opening of a fissure and possibly magma extrusion at the surface for a short time (Roult et al., 2012). Finally, as found for period B, several increases in both the number and volumes of rockfalls coincide with rainfall events (Fig. 7f). This correlation is observed between eruptions (4) and (5) and also for the rainfall peak that is synchronous with the seismic crisis that occurred between eruptions (5) and (6) for example.

5.1.4. Period D: from September 2010 to February 2011

The period from September 2010 to February 2011 was the last eruptive period considered here. The average volume of rockfalls during this period was 19 m^3 and the maximum daily average volume was 600 m^3. Two proximal, or lateral, eruptions occurred during this period on the central cone but not close to the summit. Eruption (7) occurred at the southern foot of the central cone (see Fig. 1a for location). The daily number of rockfalls increased before the onset of eruption (7) but this was not accompanied by a significant increase in the volumes of the rockfalls (Fig. 8c) nor by more intense activity, as opposed to what was found for eruptions (4), (5) and (6).

Eruption (8), which was the last eruption in the period studied, was extremely short (12 h) and was preceded by a strong displacement recorded on the east component of the SNEG GNSS station (Fig. 8e) and a smaller vertical displacement. Neither the number nor the volumes of rockfalls increased significantly before this last eruption (Fig. 8a and b). However, the activity increased markedly for several weeks after the last eruption, with a clearly visible increase in the number of rockfalls, unassociated with any increase in rainfall (Fig. 8f).

Finally, only the first seismic crisis of this period coincided with a major increase in the number of rockfalls. There was no coincident increase in rockfall volumes. This crisis was witnessed on the summit of the Piton de la Fournaise by OVPF staff who expected to observe the beginning of an eruption in the Dolomieu crater. A volcano-tectonic earthquake of magnitude 3.29 was felt during the crisis by the members of this team. The witnesses as well as a film prove that a large number of rockfalls were triggered by the earthquake. This confirms that the strongest earthquakes occurring beneath Piton de la Fournaise may trigger a series of rockfalls.

5.2. Spatial evolution

The methods presented in Hibert et al. (2014) make it possible to assess retrospectively the location and spatial distribution of the seismic energy generated by rockfalls for some specific sequences within the four periods. The spatial distribution maps of seismic energy shown in Figs. 9 and 10 were constructed by assigning the

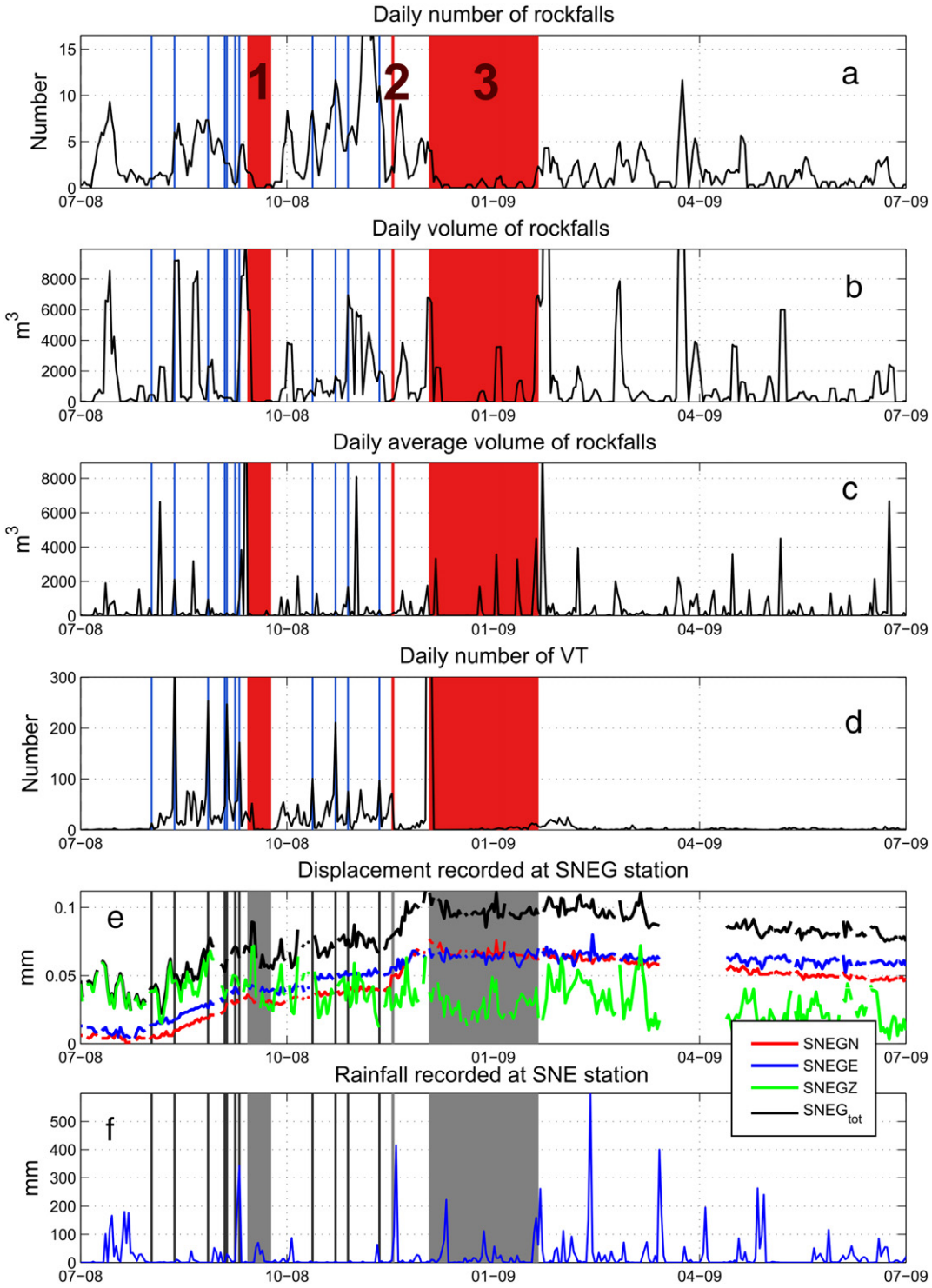

Fig. 6. a) Number of rockfalls per day for period B. Eruptions are indicated by red bars and non-eruptive seismic crises, including intrusions, by blue bars. b) Total volume of all the rockfalls that occurred on a given day. c) Daily volume divided by the daily number of rockfalls. d) Number of volcano-tectonic earthquakes per day. e) Displacements recorded by different components of the SNEG GNSS station and total displacement (black bar). f) Rainfall recorded at SNE station at the summit of Piton de la Fournaise volcano.

value of the logarithm of the seismic energy of each rockfall to circles centered on their locations. The radius of these circles has a constant value equal to the mean of the spatial error in the location of the rockfalls (180 m). This choice was made to prevent rockfalls with high location errors and large volumes from dominating this representation and to provide better visibility of all the events. The final maps are obtained by stacking all the circles corresponding to the rockfalls that occurred during the selected sequences. This representation has the advantage of integrating both the data on the number and the energy, thus providing easily interpretable information on the intensity of the rockfall activity. Finally, the horizontal displacement vectors associated with the intensity of deformation

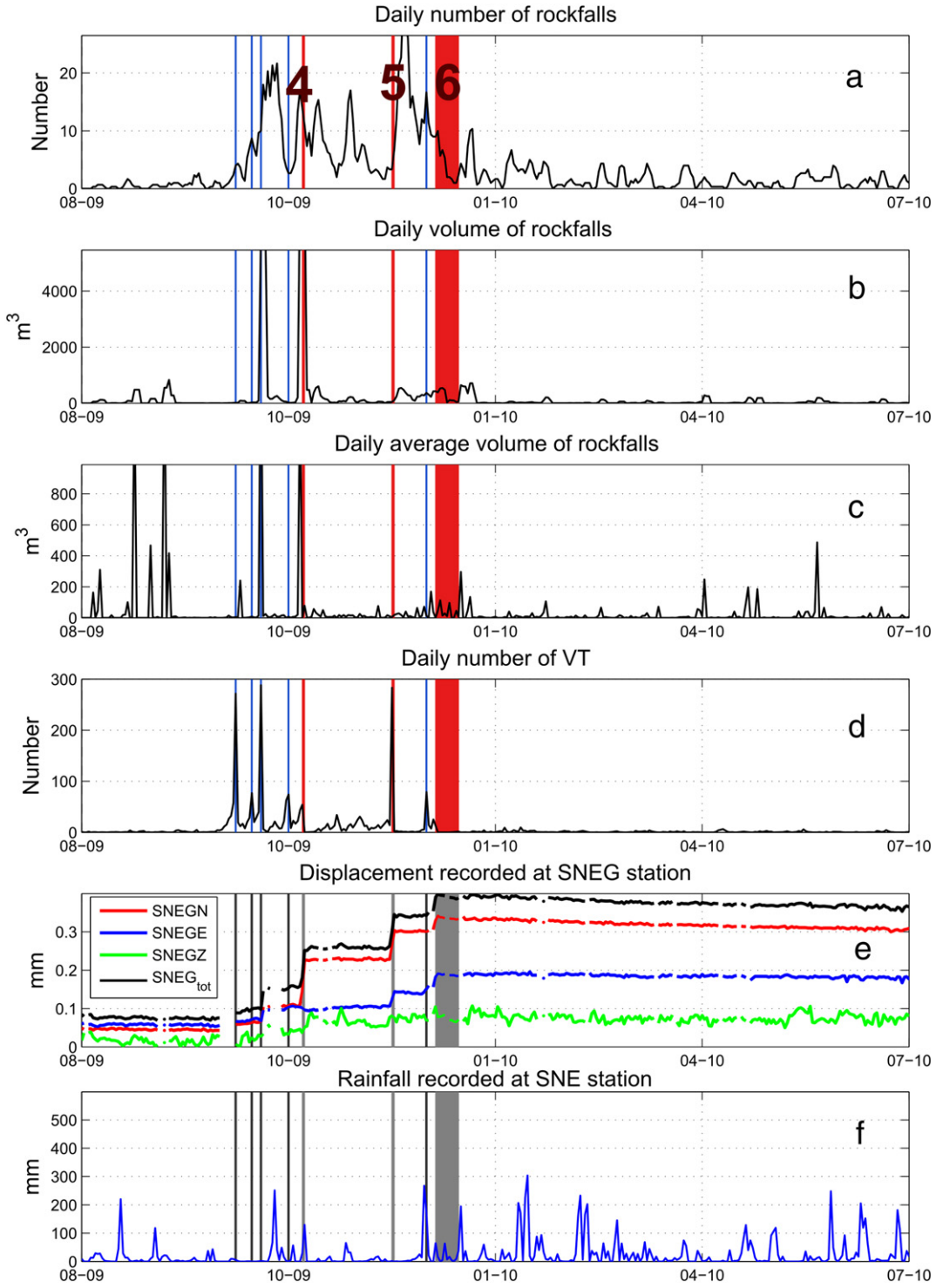

Fig. 7. a) Number of rockfalls per day for period C. Eruptions are indicated by red bars and non-eruptive seismic crises, including intrusions, by blue bars. b) Total volume of all the rockfalls that occurred on a given day. c) Daily volume divided by the daily number of rockfalls. d) Number of volcano-tectonic earthquakes per day. e) Displacements recorded by different components of the SNEG GNSS station and total displacement (in black). f) Rainfall recorded at SNE station at the summit of Piton de la Fournaise volcano.

and vertical displacements recorded at five GNSS stations near the Piton de la Fournaise summit have also been plotted to compare these data with the locations of the rockfalls.

Just after the collapse and during the following months, rockfall activity was concentrated in the south-west part of the Dolomieu crater, with a maximum intensity at the junction of the Dolomieu and Bory craters (Fig. 9b). This is consistent with the visual observations made during this period (Staudacher et al., 2009; Hibert et al., 2011), including the collapse of the detached terraces remaining after the floor collapse of the Dolomieu crater. Horizontal and vertical displacements recorded by GNSS stations show a strong subsidence of the summit, related to post-collapse relaxation.

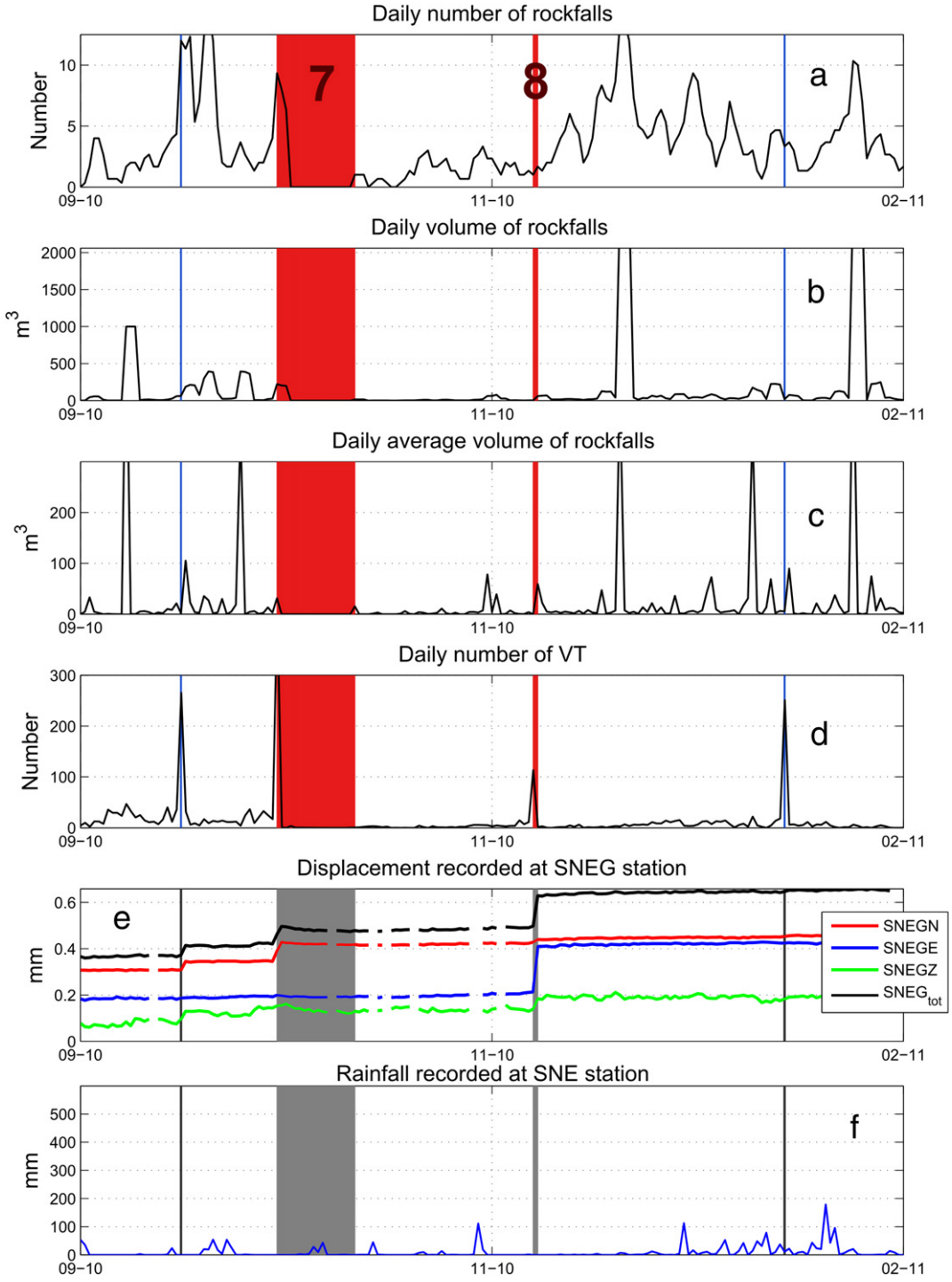

Fig. 8. a) Number of rockfalls per day for period D. Eruptions are indicated by red bars and non-eruptive seismic crises, including intrusions, by blue bars. b) Total volume of all the rockfalls that occurred on a given day. c) Daily volume divided by the daily number of rockfalls. d) Number of volcano-tectonic earthquakes per day. e) Displacements recorded by different components of the SNEG GNSS station and total displacement (in black). f) Rainfall recorded at SNE station at the summit of Piton de la Fournaise volcano.

Location maps for the events that occurred before eruption (1), between eruptions (1) and (2) and between eruptions (2) and (3) were computed. Before eruption (1), two areas of high intensity can be identified (Fig. 9c). One of these zones was near the eruptive vent of eruption (1), but also corresponded to the most unstable zone according to the activity recorded after the collapse (Fig. 9b). A second zone of high activity was located close to the area where eruption (3) subsequently occurred.

During the inter-eruptive period between eruptions (1) and (2), rockfall activity was concentrated in the south, with the highest intensity again in the south-west part of the Dolomieu crater, i.e. the area closest to the eruptive vents of these two eruptions (Fig. 9d). It is difficult to determine whether this activity concentration was a consequence of eruption (1) or a precursor of eruption (2). However, as shown by the temporal evolution, eruption (2) had no impact on the number and volumes of rockfalls. Four seismic crises also occurred

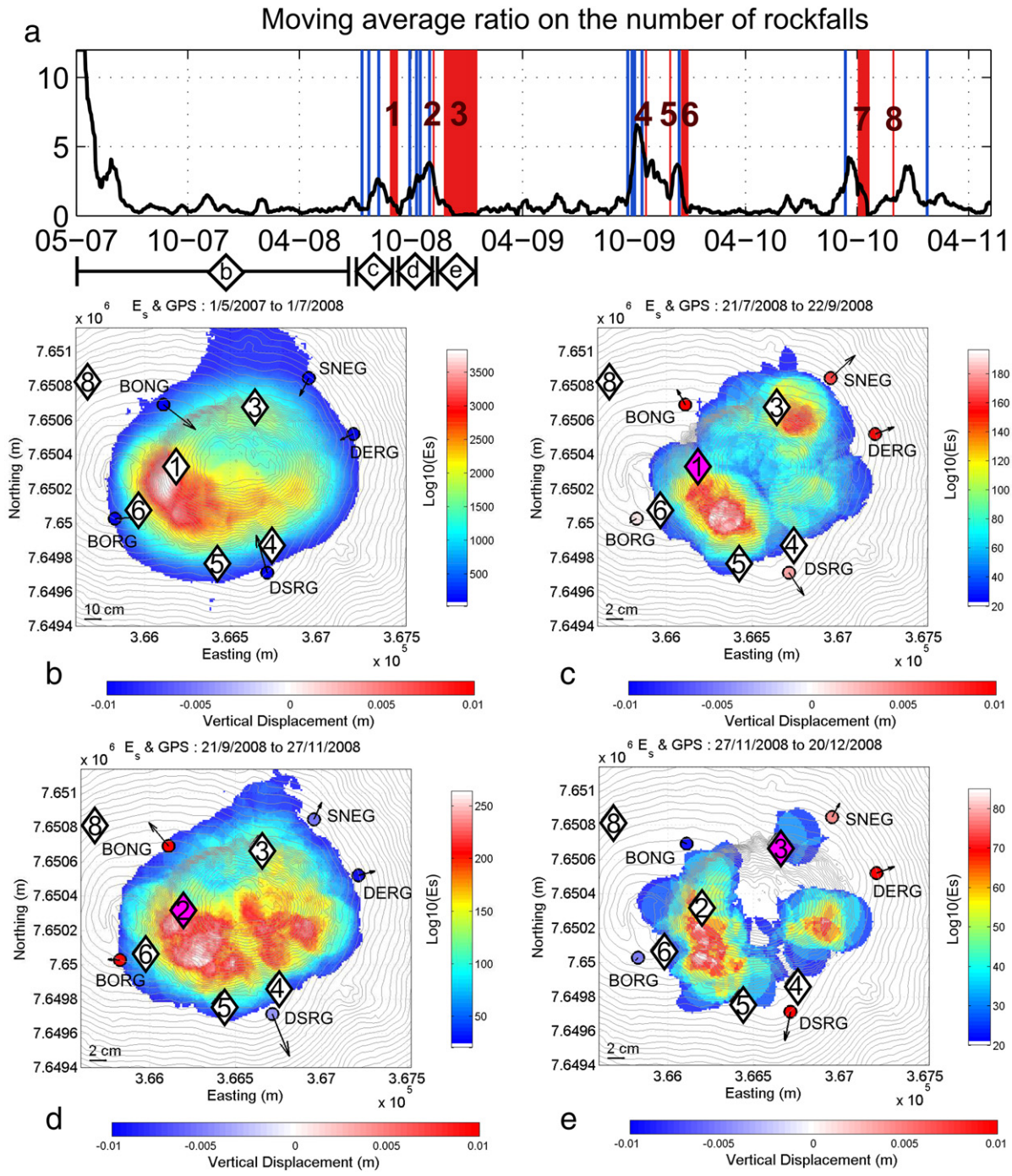

Fig. 9. a) Ratio of the moving averages (windows of 15 over 180days) of the daily number of rockfalls. Eruptions are indicated by red bars and non-eruptive seismic crises, including intrusions, by blue bars. Spatial distribution of the decimal logarithm of the seismic energy of rockfalls for the periods: b) just after the collapse; c) of 2months preceding, and the two first days of eruption (1); d) between eruptions (1) and (2), including co-eruptive deformations; e) between eruptions (2) and (3), including co-eruptive deformations. The horizontal displacement is represented by black arrows. The vertical displacement at each station is indicated by colored dots. The location of the barycentre of the eruptive fissures for each eruption is indicated by white diamonds and labeled with the number of the eruption. When an eruption occurred during the studied period, the symbols are colored in magenta.

during this inter-eruptive period and almost all had an impact on the daily number of rockfalls.

Eruptions (2) and (3) occurred 18 days apart and unfortunately we have been able to locate only a small number of rockfalls during this short period. Nevertheless, Fig. 9e shows that the activity was not concentrated in the area where eruption (3) occurred, but rather remained in the area where the maximum intensity was located between eruptions (1) and (2). A new zone of intense activity was also located on the east part of the crater, where eruption (4) occurred.

The rockfall activity preceding eruption (4) remained concentrated in the west, near the Bory crater, with another small concentration of energy close to the zone where eruption (3) occurred (Fig. 10b). For this period, the south-west quarter of the Dolomieu crater was the least affected by rockfalls. In this case, the activity of the rockfalls was concentrated in areas already destabilized by eruptions (1), (2) and (3), rather than the zone where eruption (4) occurred and where the largest deformation were recorded, as shown by the horizontal deformation on DSRG station.

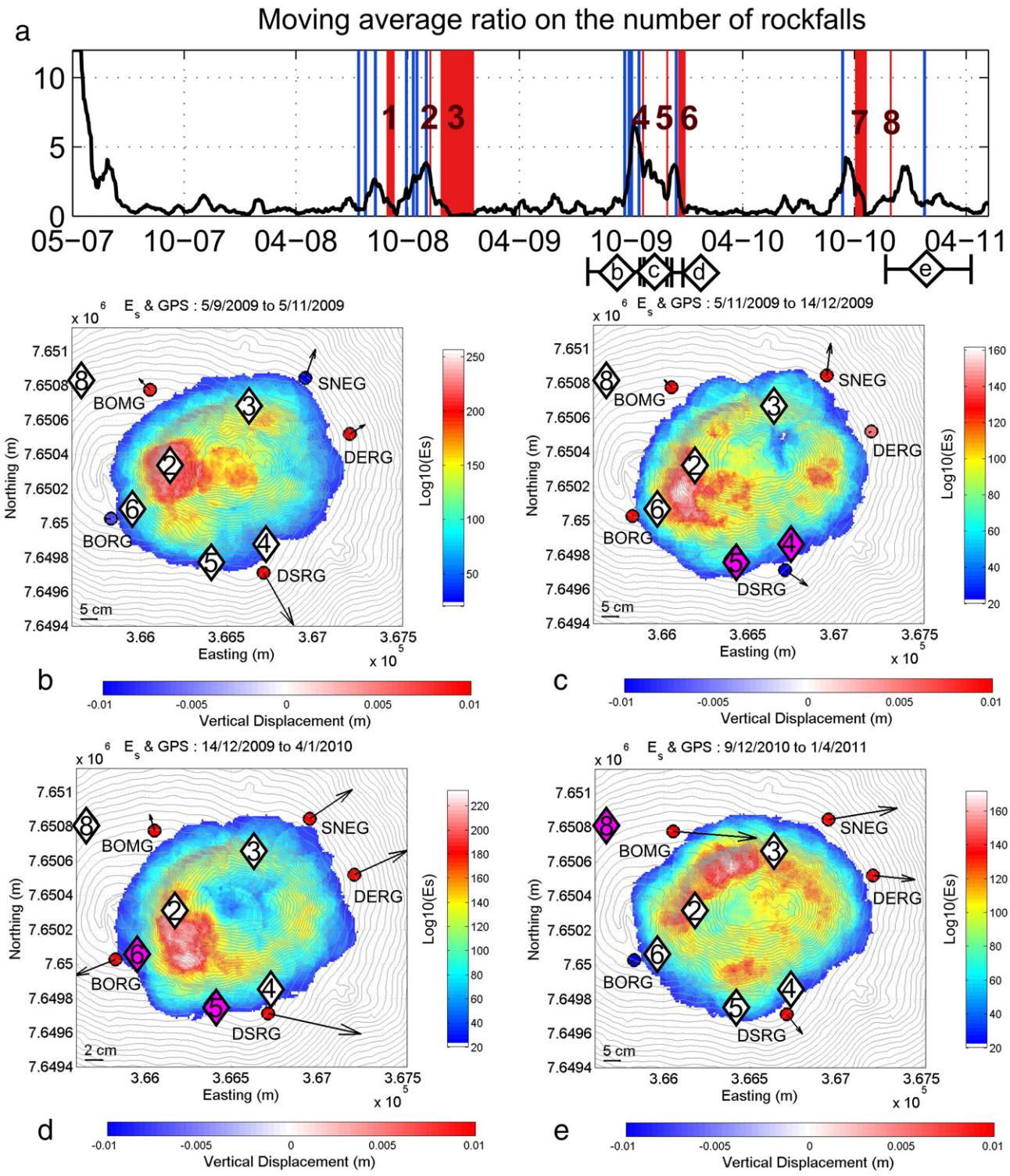

Fig. 10. a) Ratio of the moving averages (windows of 15 over 180days) of the daily number of rockfalls. Eruptions are indicated by red bars and non-eruptive seismic crises, including intrusions, by blue bars. Spatial distribution of the decimal logarithm of the seismic energy of rockfalls the periods: b) of two months before eruption (4); c) between the beginning of eruptions (4) and (5); d) between eruptions (5) and (6); e) from the beginning of eruption (8) to April 2011. The horizontal displacement is represented by black arrows. The vertical displacement at each station is indicated by colored dots. The location of the barycentre of the eruptive fissures for each eruption is indicated by white diamonds and labeled with the number of the eruption. When an eruption occurred during the studied period, the symbols are colored in magenta.

During the inter-eruptive period between eruptions (4) and (5), the rockfall activity was more intense in the southern half of the Dolomieu crater, with a maximum that remained near the Bory crater (Fig. 10c), in the area where eruption (6) occurred. There is also a small activation of a zone on the eastern side of the Dolomieu crater, close to the eruption (4) fissures.

The period following eruption (5) and before eruption (6) is characterized by a spatial concentration of rockfalls in the area bounded

to the east by the fissures of eruption (5) and to the west by the fissure of eruption (6) (Fig. 10d). Strong vertical and horizontal displacements of several centimeters were recorded at BORG, BOMG, SNEG and DERG stations (Fig. 10d). Direct observations indicate that many rockfalls occurred in the first days after the opening of eruptive fissures (6) originating from the cliff marking the boundary between the Bory and the Dolomieu craters (Hibert et al., 2015).

During the period following eruption (8), rockfall activity was once again concentrated on the western part of the Dolomieu crater, which is closer to the eruption (8) fissure (Fig. 10e). The deformation pattern presented in Fig. 10e incorporates the deformation recorded during the preparation phase of the 2 February 2011 intrusion. It shows strong deformation at BOMG, SNEG, DERG and DSRG stations, but none at BORG. This shows a decoupling between the eastern and the western part of the Piton de la Fournaise volcano, with a boundary at the junction of the Bory and Dolomieu craters, which is strongly fractured (Peltier et al., 2007, 2008, 2009a).

6. Discussion

6.1. Is their a link between rockfalls and eruptive activity?

Deciphering the relationships between the eruptive dynamics of the Piton de la Fournaise volcano and rockfall activity within the Dolomieu crater is difficult. This difficulty is mainly related to the intricate forcings that can affect Piton de la Fournaise such as seismicity, deformation and rainfall, in addition to the spontaneous collapses triggered by gravity. Moreover, the long-term post-collapse relaxation of the Dolomieu crater (Fig. 4d) produces a background noise that complicates the interpretation of the evolution of rockfall volumes within eruptive periods. In this discussion, we summarize the observations presented in the previous section (Table 2) and we assess whether interactions between eruptions, intrusions, seismic crises and rockfall activity exist and, if so, what mechanisms could explain these interactions.

Quantitatively, for 3 of the 6 summit eruptions, the number and volumes of the rockfalls increased, which was the case for only 3 of the 18 non-eruptive seismic crises and intrusions, or 2 of 18 if we consider intrusion (10) to be a special case given the observed degassing and seismic tremor that suggest arrival of magma close to the surface. Hence, the number of summit eruptions having a substantial impact on rockfall volume increases to 4 out of 7 if we considered intrusion (10) to likely be an eruption. With these considerations, only summit eruptions (2), (5) and (6) are not preceded by an increase in the volume of the rockfalls, but as stated before, eruption (2) might be a short reminiscence of eruption (1) throughout the same conduit as suggested by Peltier et al. (2010).

Proximal eruption (7) is a special case. Although some deformation was recorded at the summit, only the number of rockfalls increased and not their volumes, similar to our findings for the effect of non-eruptive seismic crises on rockfall activity. The fact that the eruptive fissure opened at the foot of the Piton de la Fournaise central cone indicates that there was probably no major local forcing at the summit, possibly explaining the lack of effect on the volume of rockfalls. During this eruption as well as during non-eruptive seismic crises, only seismic activity appears to have had an influence on rockfall activity. Similarly, eruption (8) did not occur in the immediate vicinity of the Dolomieu crater. Thus, as for eruption (7), although summit deformation was recorded, there was no direct local forcing of the incoming dike directly on the Dolomieu crater's edges.

Hence, this analysis indicates that for summit eruptions, occurring in the direct vicinity of the Dolomieu crater, both the volume and number of the rockfalls increase. For non-eruptive seismic crises and proximal or distal eruptions, only the number of rockfalls increases. This suggests that there is a link between the location of eruptive activity at the surface and the increase in rockfall volumes. We assume that the deformation caused by a dike reaching the surface and the opening of eruptive fissures can open new or extend existing fractures, resulting in the release of masses larger than those normally displaced spontaneously or released by earthquakes occurring near the Piton de la Fournaise summit. During seismic crises, the high seismicity beneath the summit may purge areas that have already been weakened. Such purging will also take place during eruptions, along with the creation and expansion of unstable areas by the deformation and the stresses imparted on the edges of the Dolomieu crater by the migration of the dike toward the surface. The lack of deformation and probably of new dike emplacement could explain why eruption (2), which opened very close to the site or eruption (1), did not have any direct impact on the rockfall activity. We did not observe any difference between the impact on the rockfall activity of the seismic crises associated with dike intrusion and the ones generated by other processes.

The spatial correlation between rockfall activity and eruptive activity is also complex. Overall, throughout the four-year period studied, rockfall activity remained the most intense in the western part of the Dolomieu crater, precisely at the junction of the Bory and Dolomieu craters. Two complementary hypotheses may be proposed to explain this observation. First, the Bory-Dolomieu junction was the most affected by the April 2007 crater floor collapse. The rims of the Bory crater were strongly weakened by the collapse of its eastern part. This made the area extremely unstable and thus prone to produce numerous rockfalls in the event of external forcings, such as deformation caused by dike migration. GNSS data reveal that a decoupling between eastward and westward deformation may have its boundary at this exact zone, thus increasing the local forcing there. Secondly, according to the location of the seismic swarms that occurred during eruptive cycles and deformation data (Peltier et al., 2008; Peltier et al., 2010; Massin et al., 2011), this high activity area is precisely above the zone from which many dikes start to migrate from the magma storage region toward the surface. For the proximal eruptions (eruptions (7) and (8)), this first phase was followed by horizontal migration at a depth ranging from 1000 to 1500 m above sea level (Fukushima et al., 2005; Peltier et al., 2007, 2008). For summit eruptions, the depth at which dikes deviate from the Bory-Dolomieu junction zone to the other parts of the Dolomieu crater is not precisely known, but is thought to be close to the surface. Thus, the dikes moving toward the summit might at first apply some local forcing on this precise zone before beginning a lateral propagation at shallow depth toward the areas where the eruptive fissure will open. This may explain why, in terms of rockfall activity, the western part of the Dolomieu crater is the most active throughout the entire period studied.

The data we gathered do not allow us to clearly identify a concentration of rockfalls in the area of an eruption in the days or weeks that precede the eruption. However, our data suggest that a concentration of rockfall activity may appear during an ongoing summit eruption in the area where a future eruption is going to occur. This was the case for the area around eruption (3), where rockfall activity was concentrated during eruptions (1) and (2) (Fig. 9c), for the area around eruption (4), where rockfalls where concentrated during a period encompassing eruptions (2) and (3) (Fig. 9d and e). This was also observed for the area around eruption (6), where rockfall activity was concentrated very close to its future eruptive fissure during the period extending from eruption (4) to eruption (5) (Fig. 10c), and after eruption (5) (Fig. 10d). The explanation we propose for this long-term trend is that a surfacing dike resulting in an eruption might not only damage the area in which it occurs, but also create weaknesses and new fractures further away. A similar mechanism of stress transfer has been observed and modeled for slow-moving landslides where ground water forcing has an impact not only in the vicinity of the water table but also further away within the landslide

Table 2
Summary of our findings concerning the relationship between rockfall activity (number per day, total volume per day and average volume on a given day) and eruptive processes (eruption, seismic crises of intrusion) given by Roult et al. (2012), seismicity and deformation recorded at SNEG station.

# Seismic crises, intrusions or eruptions (starting date)	Seismicity	Deformation recorded at SNEG	Increase in daily number of rockfalls	Increase in daily total rockfall volumes	Increase in daily avg. rockfall volumes
Seismic crisis 1 (2008/8/4)	Weak	None	No	No	No
***Seismiccrisis2* (2008/8/15)**	Strong	Slow	Yes	Yes	Yes
Seismic crisis 3 (2008/8/31)	Strong	Slow	No	Yes	No
Seismic crisis 4 (2008/09/07)	Weak	Slow	Yes	No	No
Intrusion 1 (2008/09/08)	Strong	Slow	Yes	No	No
Intrusion 2 (2008/09/12)	Weak	Slow	No	No	No
***Seismiccrisis5* (2008/09/15)**	Strong	Slow	Yes	Yes	Yes
***Eruption1* (2008/9/21)**	Weak	Slow	Yes	Yes	Yes
Intrusion 3 (2008/10/20)	Weak	None	Yes	No	No
Intrusion 4 (2008/10/31)	Strong	None	Yes	No	No
Seismic crisis 6 (2008/11/6)	Weak	None	No	Yes	No
Seismic crisis 7 (2008/11/20)	Weak	None	Yes	No	No
Eruption 2 (2008/11/27)	Weak	None	No	No	No
***Eruption3* (2008/12/15)**	Strong	Slow	Yes	Yes	Yes
Intrusion 5 (2009/10/7)	Strong	None	Yes	No	No
Seismic crisis 8 (2009/10/14)	Weak	None	Yes	No	No
***Intrusion°6* (2009/10/18)**	Strong	Fast	Yes	Yes	Yes
Seismic crisis 9 (2009/10/30)	Weak	None	No	No	No
***Eruption4* (2009/11/5)**	Weak	Fast	Yes	Yes	Yes
Eruption 5 (2009/12/14)	Strong	Fast	No	No	No
Seismic crisis 10 (2009/12/29)	Weak	None	No	No	No
Eruption 6 (2010/1/2)	Weak	Fast	No	No	No
Intrusion 7 (2010/9/23)	Strong	Fast	Yes	No	No
Eruption 7 (2010/10/14)	Strong	Fast	Yes	No	No
Eruption 8 (2010/12/9)	Weak	Fast	No	No	Yes
Seismic crisis 11 (2011/2/6)	Strong	None	Yes	No	Yes

Eruptions, seismic crises or intrusions for which the daily number, daily total volumes and daily average volumes of rockfalls increased significantly in the preceding days are indicated in **bold**. Intrusion (6) is a special case as degassing was observed at the top of the central cone of Piton de la Fournaise volcano and seismic tremor recorded, suggesting activity at the surface. However no lava flow was observed, hence the intrusion qualification for this event.

(e.g. Cappa et al., 2014). This fracturing might lead to an intensification of rockfall activity in the affected area and create, at depth, a preferred path taken by the future dike when it deviates from the Bory-Dolomieu junction to reach the surface. Thus, the zone where rockfall activity is intensified during a given summit eruption might indicate where the next summit eruption will occur.

6.2. Rockfalls and rainfalls

Several peaks in rockfall activity coincide with peaks of rainfall recorded at the summit of Piton de la Fournaise. To better understand the relationships involved, we compared the times series of rainfall recorded at SNE station and the number and volumes of rockfalls. It is very difficult to objectively quantify this interaction from Figs. 5, 6, 7 and 8. To overcome this difficulty, we used the following approach. Each rainfall peak exceeding a threshold of 50 mm per day was identified. We then looked at the cross-correlation between the time series of the rockfall volume, the number of rockfalls and rainfall ranging from 5 days before to 1 day after the day of the identified rainfall peak. The cross-correlation was calculated several times, shifting one of the time series by one day. This allowed us to identify the time lag that gave the best correlation. Finally, the time series were normalized so that if they were identical for a given offset, the value of the cross-correlation was 1.

By applying this strategy, we identified 94 rainfall peaks exceeding 50 mm per day. 53% of these peaks showed a correlation with the volume curve exceeding 0.5, 51% exceeding 0.70 and 23% exceeding 0.9. The average value of the offsets corresponding to these best correlations (0.9) is 0.8 day. The same processing was used to compare the daily number of rockfalls and rainfall. The correlation between the daily number of rockfalls and rainfall was higher than 0.5 for 49% of the peaks, higher than 0.7 for 44% of the peaks and higher than 0.9 for 16% of the peaks. The average value of the offsets corresponding to these best correlations is 0.7 day.

Thus, for some cases, there is a correlation between rainfall and the triggering of rockfalls, however the correlation is not systematic. The response time between the arrival of an intense rainfall and an increase in the intensity of the rockfall activity is very short. The extreme fracturation of the surface explains the fast infiltration and associated mechanical responses, such as the triggering of rockfalls. Finally, the proportion of strong correlations between the peaks of the rainfall curve and the volume of rockfalls is higher than that obtained for the correlation with the daily number of rockfalls. This suggests that the intense rainfalls have a greater impact on the volume than on the number of rockfalls they trigger.

Finally, we tried to determine whether or not a rainfall threshold existed to trigger a peak in rockfall activity (number or volume). We computed the cumulative sum of the rainfall over the days before each of the peaks of correlation between the rainfall and the number

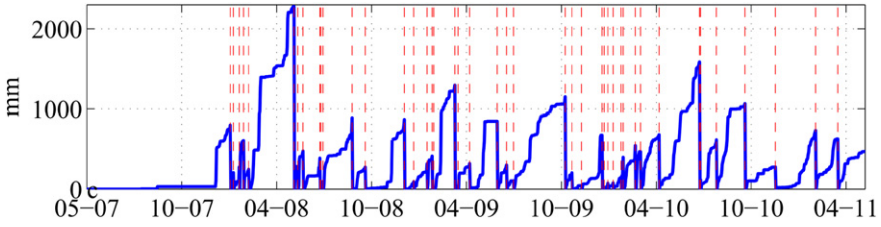

Fig. 11. Cumulative sum of rainfall before each correlated peak of number of rockfalls (at times indicated by the red dotted lines).

or the volume of rockfalls with values exceeding 0.70. No threshold was found (Fig. 11). Some peaks in rockfall activity are correlated with peaks of rainfall corresponding to cumulative amounts of rain ranging from 50 mm in 1 day to 2300 mm in 88 days. The absence of a threshold suggests that the triggering of rockfalls by rainfall could be the result of an intense and immediate forcing rather than the loading of the material with water to a certain threshold. This may be linked to the fact that the Dolomieu crater and its vicinity are extremely fractured.

7. Conclusion

The results presented in this study highlight the very complex links between the external forcing and rockfall activity at the Piton de la Fournaise volcano during the four years that followed the collapse of the Dolomieu crater floor. Besides the direct impact of the Dolomieu crater floor collapse, three main forcings are identified as capable of impacting the daily number and volume of rockfalls: i) local surface deformation of the summit related to dike migration, ii) local seismicity and iii) intense rainfall events.

Our analysis reveals that the impact of the April 2007 Dolomieu crater floor collapse on rockfall activity can be separated into two phases. During the first phase directly following the collapse, the most intense rockfall activity occurred. During this period, lasting three months from May 2007 to July 2007, both the daily number and volume of rockfalls decreased sharply from the initially high values. After this period, a second and slower phase of relaxation, lasting from August 2007 to January 2010, was characterized by a decrease in the daily volume of the rockfalls while their daily number remained almost constant. This observation suggests that the purge of the unstable zones created by the Dolomieu crater floor collapse, while extremely intense in the months after the collapse, took almost two and a half years to complete.

On the time scales of months, the intensity of the rockfall activity almost always increases during eruptive cycles. When looking in detail at the volcanic processes within an eruptive cycle, we observe a difference between the impact of summit eruptions and the impact of non-eruptive seismic crises or more distal eruptions on rockfall activity. The strong earthquakes occurring below the summit of Piton de la Fournaise affect rockfall activity by increasing their number. This is particularly true when a large number of high-magnitude volcano-tectonic earthquakes are observed during a seismic crisis. When a dike reaches the surface, producing an eruption, the daily total and daily average volumes of rockfalls increase. The increase in the volume of rockfalls is observed for the majority of summit eruptions but not for the eruptions that occurred on the slope or at the foot of the central cone and not for intrusions (when the dike does not reach the surface). For both non-eruptive seismic crises or eruptions that do not occur in the vicinity of the Dolomieu crater, the increase in the number of rockfalls without an increase in their volumes can be explained by the purge of already existing unstable areas by the strong seismicity.

For the summit eruptions, the local forcing of the migrating dike reaching the surface and the opening of eruptive fissures close to or within the Dolomieu crater may create and destabilize new areas, which may explain why we find an increase in the volume of the rockfalls and not only in their number. The areas where rockfall activity intensifies are not in the vicinity of the eruptive fissures of the ongoing eruption, but rather in the areas where the following eruption is going to occur. This observation suggests that a summit eruption will not only affect its direct surrounding but will also affect other areas in the vicinity of the Dolomieu crater. These newly created weak zones are prone to produce voluminous and numerous rockfalls, but will also become preferred paths for future dikes to reach the surface. Therefore, the localization of the intensification of the rockfall activity during an ongoing summit eruption might indicate in which areas the next summit eruption will occur.

Finally, the intense rainfall events that occur on La Réunion Island also have an influence on the intensity of rockfall activity, resulting in an increase in the number as well as in the volume of rockfalls. The impact of rainfall seems to be more the result of a fast destabilization rather than a continuous loading of the materials, since no threshold could been found. Such a fast hydrological mechanism can destabilize larger volumes, leading to the fast displacement of unstable areas that normally would have taken longer to collapse spontaneously.

Our study sheds light on the complex interaction between volcanic and rockfall activities. The correlations we observed suggest that rockfall activity may carry important information on the local deformation that occurs close the Piton de la Fournaise summit and that might indicate whether a magma propagation within the edifice will reach the surface or not, giving insight on whether a seismic crisis will be followed by an eruption or not. However, before considering rockfalls as a precursor of summit eruptions at Piton de la Fournaise, several issues must be addressed, opening new perspectives for future studies. In particular, the triggering of rockfalls by local volcano-tectonic earthquakes must be more thoroughly investigated by looking in detail at known sequences of the two types of events and assessing whether or not volcano-tectonic earthquakes magnitude or depth thresholds exist for rockfall triggering. Rockfall activity at Piton de la Fournaise is also constantly evolving and its interaction with volcanic activity may change over time, especially with the constant purge of the areas destabilized by the April 2007 Dolomieu crater floor collapse. Hence more studies must be carried out for more recent periods to confirm our observations focused on the four years directly following the Dolomieu crater floor collapse.

Acknowledgment

This study is part of the ANR_08_RISK_011/UnderVolc project and was supported by grants from the French Agence Nationale de la Recherche (ANR), BRGM and ERC contract ERCCG-2013-PE10-617472 SLIDEQUAKES. We want to thank Thomas Dewez for the help and support he provided in the building of the seismically triggered camera devices. We are very grateful to Philippe Catherine and Frédérique Lauret for their support in the field and their help in providing high quality data. We would like to thank in particular Geneviéve Roult and Benoit Taisne for their very fruitful discussions and the assistance they provided. The authors gratefully acknowledge two anonymous reviewers for their insightful reviews and the editor who helped to greatly improve this manuscript.

References

Acocella, V., Neri, M., Scarlato, P., 2006. Understanding shallow magma emplacement at volcanoes: orthogonal feeder dikes during the 2002–2003 Stromboli (Italy) eruption. Geophys. Res. Lett. 33, L17310. http://dx.doi.org/10.1029/2006GL026862.

Allen, R., 1982. Automatic phase pickers: their present use and future prospects. Bull. Seismol. Soc. Am. Vol. 72 (6), S225–S242.

Bachèlery, P., 1981. Le Piton De La Fournaise (Ile De La Réunion), Etude Volcanologique, Structurale Et PéTrologique. Univ. Clermont-Ferrand II, France. Ph.D. Thesis

Bachèlery, P., Saint-Ange, F., Villeneuve, N., Savoye, B., Normand, A., Le Drezen, E., Barrère, A., Quod, J.P., Deplus, C., 2010. Huge Lava Flows into the Sea and Caldera Collapse, April 2007, Piton de la Fournaise volcano. In IAVCEI Third Workshop on Collapse Calderas. La Ré,union, , pp. 3–9. October

Baillard, C., Crawford, W.C., Ballu, V., Hibert, C., Mangeney, A., 2014. An automatic kurtosis-based P-and S-phase picker designed for local seismic networks. Bull. Seismol. Soc. Am. 104 (1), 394–409.

Battaglia, J., Ferrazzini, V., Staudacher, T., Aki, K., Cheminée, J.L., 2005. Pre-eruptive migration of earthquakes at the Piton de la Fournaise volcano (réunion Island). Geophys. J. Int. 161 (2), 549–558.

Bonaccorso, A., Calvari, S., Garfi, G., Lodato, L., Patane, D., 2003. Dynamics of the December 2003 flank failure and tsunami at Stromboli volcano inferred by volcanological and geophysical observations. Geophys. Res. Lett. 30 (18), 1941. http://dx.doi.org/10.1029/2003GL17702.

Calder, E.S., Luckett, R., Sparks, R.S.J., Voight, B., 2002. Mechanisms of lava dome instability and generation of rockfalls and pyroclastic flows at Soufriére Hills volcano, Montserrat. In: Druitt, T.H., Kokelaar, B.P. (Eds.), The Eruption of Soufrieére Hills Volcano, Montserrat, from 1995 to 1999. Geol. Soc. London Mem. 21. pp. 483–516.

Calder, E.S., Cortes, J.A., Palma, J.L., Luckett, R., 2005. Probabilistic analysis of rockfall frequencies during an andesite lava dome eruption: the Soufrière Hills Volcano, Montserrat. Geophys. Res. Letters 32, L16309. http://dx.doi.org/10.1029/2005GL023594.

Calvari, S., Spampinato, L., Lodato, L., Harris, A.J.L., Patrick, M.R., Dehn, J., Burton, M.R., Andronico, D., 2005. Chronology and complex volcanic processes during the 2002–2003 flank eruption at Stromboli volcano (Italy) reconstructed from direct observations and surveys with a handheld thermal camera. J. Geophys. Res. 110, 1029/2004JB003129.

Cappa, F., Guglielmi, Y., Viseur, S., Garambois, S., 2014. Deep fluids can facilitate rupture of slow moving giant landslides as a result of stress transfer and frictional weakening. Geophys. Res. Lett. 41 (1), 61–66.

Collombet, M., Grasso, J.R., Ferrazzini, V., 2003. Seismicity rate before eruptions on Piton de la Fournaise volcano: implications for eruption dynamics. Geophys. Res. Lett. 30 (21), 2099.

Crampin, S., Båth, M., 1965. Higher modes of seismic surface waves: mode separation. Geophys. J. Int. 10 (1), 81–92.

Deniel, C., Kieffer, G., Lecoindre, J., 1992. New 230Th–238U and 14C age determinations from Piton des Neiges volcano, Reunion — a revised chronology for the differentiated series. J. Volcanol. Geotherm. Res. 51, 253–267.

Di Muro, A., Staudacher, T., Ferrazzini, V., Métrich, N., Besson, P., Garofalo, C., Villemant, B., 2015. Shallow magma storage at Piton de la Fournaise volcano after 2007 summit caldera collapse tracked in Pele's hairs. *Hawaiian volcanoes: from source to surface*. Geophys. Monogr. Ser. 208, 189–212.

Dupon, J.F., 1984. Landslides and Mudflow in a Young Volcanic Hawaiian Type Structure, Rapport de l'Office de la Recherche Scientifique et Technique d'Outre-Mer P'apeete. Tahiti.

Duncan, R.A., 1981. Hotspots in the southern oceans - an absolute frame of reference for motion of the Gondwana continents. Tectonophysics 74, 24–29.

Falsaperla, S., Neri, M., Pecora, E., Spampinato, S., 2006. Multidisciplinary study of flank instability phenomena at Stromboli volcano, Italy. Geophys. Res. Letters 33, L09304. http://dx.doi.org/10.1029/2006GL025940.

Falsaperla, S., Neri, M., Pecora, E., Spampinato, S., 2008. Can flank instability at Stromboli volcano provide insights into precursory patterns of eruptions? http://eartprints.org.

Fukushima, Y., Cayol, V., Durand, P., 2005. Finding realistic dike models from interferometric synthetic aperture radar data: the February 2000 eruption at Piton de La Fournaise. J. Geophys. Res. 110, B03206. http://dx.doi.org/10.1029/2004JB003268.

Hibert, C.A., Mangeney, A., Grandjean, G., Shapiro, N., 2011. Slope instabilities in Dolomieu crater, Reunion Island: from seismic signals to rockfall characteristics. J. Geophys. Res. 116, F04032. http://dx.doi.org/10.1029/2011JF002038.

Hibert, C.A., Mangeney, A., Grandjean, G., Baillard, C., Rivet, D., Shapiro, N.M., Satriano, C., Maggi, A., Boissier, P., Ferrazzini, V., Crawford, W., 2014a. Automated identification, location, and volume estimation of rockfalls at Piton de la Fournaise volcano. J. Geophys. Res. Earth Surf. 119 (5), 1082–1105.

Hibert, C.A., Mangeney, A., Polacci, M., Ferrazzini, V., Dimuro, A., Vergniolle, S., Peltier, A., Grandjean, G., Dewez, T., Taisne, B., Burton, M., Staudacher, T., Brenguier, F., Dupont, A., Kowalski, P., Boissier, P., Catherine, P., Lauret, F., 2015. Towards continuous quantification of lava extrusion rate: results from the multidisciplinary analysis of the 2 January 2010 eruption of Piton de la Fournaise volcano, La Runion. J. Geophys. Res. Solid Earth. 120,

Hirata, T., 1987. Omori's power law aftershock sequences of microfracturing in rock fracture experiment. J. Geophys. Res. Solid Earth 92 (B7), 6215–6221.

Kanamori, H., Given, J.W., 1982. Analysis of long-period seismic waves excited by the May 18,1980, eruption of Mount St-Helens – a terrestrial monopole. J. Geophys. Res. 87, 5422–5432.

Kanamori, H., Given, J.W., Lay, T., 1984. Analysis of seismic body waves excited by the mount St-Helens eruption of May 18, 1980. J. Geophys. Res. 89, 1856–1866.

La Rocca, M., Galluzzo, D., Saccorotti, G., Tinti, S., Cimini, G.B., Del Pezzo, E., 2004. Seismic signals associated with landslides and with a tsunami at Stromboli volcano, Italy. Bull. Seism. Soc. Am. 94 (5), 1850–1867.

Lengliné, O., Marsan, D., Got, J.L., Pinel, V., Ferrazzini, V., Okubo, P.G., 2008. Seismicity and deformation induced by magma accumulation at three basaltic volcanoes. J. Geophys. Res. Solid Earth (1978–2012) 113 (B12).

Marc, O., Hovius, N., Meunier, P., Uchida, T., Hayashi, S., 2015. Transient changes of landslide rates after earthquakes. Geology 43 (10), 883–886.

Massin, F., Ferrazzini, V., Bachèlery, P., Nercessian, A., Duputel, Z., Staudacher, T., 2011. Structures and evolution of the plumbing system of Piton de la Fournaise volcano inferred from clustering of 2007 eruptive cycle seismicity. J. Volcanol. Geotherm. Res. 202 (1), 96–106.

Michon, L., Staudacher, T.h., Ferrazzini, V., Bachelery, P., Marti, J., 2007. April 2007 collapse of Piton de la Fournaise: a new example of caldera formation. Geophys. Res. Lett. 34 (L21301). http://dx.doi.org/10.1029/2007GL031248.

Michon, L., Di Muro, A., Villeneuve, N., Saint-Marc, C., Fadda, P., Manta, F., 2013. Explosive activity of the summit cone of Piton de la Fournaise volcano (La Réunion island): a historical and geological review. J. Volcanol. Geotherm. Res. 264, 117–133.

Mueller, S.B., Varley, N.R., Kueppers, U., Lesage, P., Davila, G.A.R., Dingwell, D.B., 2013. Quantification of magma ascent rate through rockfall monitoring at the growing/collapsing lava dome of Volcn de Colima, Mexico. Solid Earth 4 (2), 201.

Orr, T.R., Thelen, W.A., Patrick, M.R., Swanson, D.A., Wilson, D.C., 2013. Explosive eruptions triggered by rockfalls at Kilauea volcano, Hawaii. Geology 41 (2), 207–210.

Peltier, A., Ferrazzini, V., Staudacher, T., Bachèlery, P., 2005. Imaging the dynamics of dyke propagation prior to the 2000–2003 flank eruptions at Piton de La Fournaise, Reunion Island. Geophys. Res. Lett. 32 (22).

Peltier, A., Staudacher, T., Bachélery, P., 2007. Constraints on magma transfers and structures involved in the 2003 activity at Piton de La Fournaise from displacement data. J. Geophys. Res. Solid Earth (1978–2012) 112 (B3).

Peltier, A., Famin, V., Bachèlery, P., Cayol, V., Fukushima, Y., Staudacher, T., 2008. Cyclic magma storages and transfers at Piton de La Fournaise volcano (La réunion hotspot) inferred from deformation and geochemical data. Earth Planet. Sci. Lett. 270 (3), 180–188.

Peltier, A., Bachelery, P., Staudacher, T., 2009a. Magma transport and storage at Piton de La Fournaise (La réunion) between 1972 and 2007: a review of geophysical and geochemical data. J. Volcanol. Geotherm. Res 184, 93–108.

Peltier, A., Staudacher, T., Bachelery, P., Cayol, V., 2009b. Formation of the April 2007 caldera collapse at Piton de La Fournaise volcano: insights from GPS data. J. Volcanol. Geotherm. Res. 184, 152–163. http://dx.doi.org/10.1016/j.jvolgeores.2008.09.009.

Peltier, A., Staudacher, T., Bachelery, P., 2010. New behaviour of the Piton de La Fournaise volcano feeding system (La Réunion Island) deduced from GPS data: influence of the 2007 Dolomieu caldera collapse. J. Volcanol. Geotherm. Res. 192 (1), 48–56.

Peltier, A., Massin, F., Bachèlery, P., Finizola, A., 2012. Internal structure and building of basaltic shield volcanoes: the example of the Piton de La Fournaise terminal cone (La Réunion). Bull. Volcanol. 74 (8), 1881–1897.

Rousseau, N., 1999. Study of Seismic Signal Associated with Rockfalls at 2 Sites on the Réunion Island (Indian Ocean): Mahavel Cascade and Soufrière cavity. Doctoral Thesis of the Institut de Physique du Globe de Paris, 134 pp

Roult, G., Peltier, A., Taisne, B., Staudacher, T., Ferrazzini, V., Di Muro, A., The OVPF Team, 2012. A new comprehensive classification of the Piton De La Fournaise activity spanning the 1985–2010 Period. Search and analysis of short-term precursors from a broad-band seismological station. J. Volcanol. Geotherm. Res. 241, 78–104. http://dx.doi.org/10.1016/j.jvolgeores.2012.06.012.

Sethian, J.A., 1996a. A fast marching level set method for monotonically advancing front. Proc. Nat. Acad. Sci. 93, 1591–1595.

Sethian, J.A., 1996b. Theory, algorithms, and applications of level set methods for propagating interfaces. Acta Numerica 5, 309–395.

Sethian, J.A., 1996c. Level set methods. Cambridge Univ. Press.

van Trier, J., Symes, W., 1991. Upwind finite difference compulation of traveltimes. Geophysics 56, 812–821.

Stieltjes, L., 1990. Evaluation Des Risques Naturels Au Piton De La Fournaise. In: Lénat, J. (Ed.), Le volcanisme de la Reùnion - Monographie. Clermont-Ferrand, Centre de Recherche en Volcanologie, pp. 357–379.

Staudacher, 2010. Field observations of the 2008 summit eruptions at Piton de la Fournaise (Ile de La Réunion) and implications on the 2007 Dolomieu collapse. J. Volcanol. Geortherm. Res. 198, 60–68.

Staudacher, T., Ferrazzini, V., Peltier, A., Kowalski, P., Boissier, P., Catherine, P., Lauret, F., Massin, F., 2009. The April 2007 eruption and Dolomieu crater collapse, two major events at Piton de la Fournaise (La Réunion Island). J. of Volcanol. Geotherm. Res. 184, 126–137.

Taisne, B., Brenguier, F., Shapiro, N.M., Ferrazzini, V., 2011. Imaging the dynamics of magma propagation using radiated seismic intensity. Geophys. Res. Lett. 38 (4).

Ui, T., Matsuwo, N., Sumita, M., Fujinawa, A., 1999. Generation of block and ash flows during the 1990–1995 eruption of Unzen Volcano, Japan. J. Volcanol. Geotherm. Res. 89, 123–137.

Urai, M., Geshi, N., Staudacher, T.h., 2007. Size and volume evaluation of the Caldera collapse on Piton de la Fournaise volcano during the April 2007 eruption using ASTER stereo imagery. Geophys. Res. Lett. 34 (L22318). http://dx.doi.org/10.1029/2007GL031551.

Vilajosana, I., Surinach, E., Abellán, A., Khazaradze, G., Garcia, D., Llosa, J., 2008. Rockfall induced seismic signals: case study in Montserrat, Catalonia. Nat. Hazards Earth Syst. Sci. 8 (4), 805–812.

Voight, B., Sparks, R.S.J., Miller, A.D., Stewart, R.C., Hoblitt, R.P., Clarke, A., Ewart, J., Aspinall, W.P., Baptie, B., Calder, E.S., Cole, P., Druitt, T.H., Hartford, C., Herd, R.A., Jackson, P., Lejeune, A.M., Lockhart, A.B., Loughlin, S.C., Luckett, R., Lynch, L., Norton, G.E., Robertson, R., Watson, I.M., Watts, R., Young, S.R., 1999. Magma flow instability and cyclic activity at Soufrière Hills Volcano, Montserrat, British West Indies. Science 283 (5405), 1138–1142.

Voight, B., Yound, K.D., Hidayat, D., Subandrio, M.A., Ratdomopurbo, A., Suharna, p., Sayudi, D.S., LaHusen, R., Marso, J., Murray, T.L., Dejean, M., Igushi, M., Ishiara, K., 2000. Purbawianata Deformation and seismic precursors to dome-collapse and fountain-collapse nuées ardentes at Merapi Volcano, Java, Indonesia, 1994–1998. J. of Volcanol. And Geotherm. Res. 100, 261–287.

Watts, R.B., et al. 2001. Growth patterns and emplacement of the andesitic lava dome at Soufrière Hills volcano, Montserrat. In: Druitt, T.H., Kokelaar, B.P. (Eds.), The Eruption of Soufrière Hills Volcano, Montserrat, from 1995 to 1999. Geol. Soc. London Mem. 21. pp. 115–152.

Wieczorek, G.F., Nishenko, S.P., Varnes, D.J., 1995. Analysis of Rock Falls in the Yosemite Valley, California. In: Daemen, J., Schultz, R.A. (Eds.), In 35th US Symposium on Rock Mechanics. pp. 85–89. June.

Zobin, V.M., Varley, N.R., González, M., Orozco, J., Reyes, G.A., Navarro, C., Bretón, M., 2008. Monitoring the 2004 andesitic block-lava extrusion at Volcán de Colima, México from seismic activity and SO2 emission. J. Volcanol. Geotherm. Res. 177 (2), 367–377.